

1 **Running title:** Evolution of Plant Cysteine Oxidases

2

3 **Corresponding author:**

4 Francesco Licausi

5 Department of Plant Sciences

6 University of Oxford

7 South Park Rd

8 OX1 3RB Oxford, United Kingdom

9

10 **Title:** Acquisition of hypoxia inducibility by oxygen sensing N-terminal cysteine oxidase in  
11 spermatophytes

12

13 **Authors:** Daan A. Weits<sup>1,2</sup>, Lina Zhou<sup>1,3,4</sup>, Beatrice Giuntoli<sup>2,5</sup>, Laura Dalle Carbonare<sup>2</sup>, Sergio  
14 Iacopino<sup>5,6</sup>, Luca Piccinini<sup>2</sup>, Vinay Shukla<sup>2</sup>, Liem T. Bui<sup>2</sup>, Giacomo Novi<sup>2</sup>, Joost T. van Dongen<sup>1</sup> &  
15 Francesco Licausi<sup>2,5,6</sup>

16 <sup>1</sup> Institute of Biology, RWTH Aachen University, Aachen, 52074, Germany

17 <sup>2</sup> Institute of Life Sciences, Scuola Superiore Sant'Anna, Pisa, 56124, Italy

18 <sup>3</sup> School of Life Sciences, Lanzhou University, Lanzhou, 730000, People's Republic of China

19 <sup>4</sup> School of Ecology and Environment, Northwestern Polytechnical University, Xi'an 710072, China

20 <sup>5</sup> Biology Department, University of Pisa, Pisa, 56127, Italy

21 <sup>6</sup> Department of Plant Sciences, University of Oxford, Oxford, OX1 3RB, United Kingdom

22

23 **One sentence summary:**

24 Hypoxic induction of Plant Cysteine Oxidases has been acquired and fixed in seed plants by  
25 ancestor proteins able to initiate the proteolysis of Cys-initiating protein substrates by the Arg/N-  
26 degron pathway.

27

28 **Footnotes**

29 **Author contributions:** D.A.W., B.G., J.v.D and F.L., conceived, designed and coordinated the  
30 experiments. D.A.W, L.T.B., L.Z., L.P., L.D.C., V.S. and F.L. performed the experiments. G.N.  
31 produced the genotypes used in the current study. F.L., D.W. and S.I. performed phylogenetic  
32 analyses. F.L. and D.A.W. wrote the manuscript. All authors read and approved the final  
33 manuscript.

34 **Funding:** Results have been achieved within the framework of the PRIN2017 project  
35 20173EWR9 funded by the Italian Ministry of University and Research. Lina Zhou was  
36 financially supported by the China Scholarship Council.

37

38 **Corresponding author e-mail:** [francesco.licausi@plants.ox.ac.uk](mailto:francesco.licausi@plants.ox.ac.uk)

39

40

41 **Abstract**

42

43 N-terminal cysteine oxidases (NCOs) are enzymes that use molecular oxygen to oxidize the amino-  
44 terminal cysteine of specific proteins, thereby initiating the proteolytic N-degron pathway and thus  
45 conferring them oxygen-dependent instability. To expand the characterization of the plant family of  
46 NCOs (PCOs), we performed a phylogenetic analysis across different plant taxa in terms of  
47 sequence similarity and transcriptional regulation. Based on this survey, we propose a distinction of  
48 PCOs into two main groups: A-type and B-type sequences. A-type PCOs are conserved across all  
49 plant species and are generally unaffected at the mRNA level by oxygen availability. Instead, B-  
50 type PCOs differentiated in spermatophytes to acquire specific amino acid features and  
51 transcriptional regulation in response to hypoxia. Both groups of PCO proteins possess the ability to  
52 destabilize Cys-initiating proteins. Indeed, the inactivation of two A-type PCOs in *Arabidopsis*  
53 *thaliana*, PCO4 and PCO5, is sufficient to activate, at least partially, the anaerobic response in  
54 young seedlings, whereas the additional removal of B-type PCOs leads to a stronger induction of  
55 anaerobic genes and impairs plant growth and development. Our results show that both PCO types  
56 are required to regulate the anaerobic response in angiosperm. Therefore, while it is possible to  
57 distinguish two clades within the PCO family, separated by both amino acid features and  
58 transcriptional regulation, we conclude that they both contribute to restrain the anaerobic  
59 transcriptional program in normoxic conditions and together generate a molecular switch to toggle  
60 the hypoxic response in *Arabidopsis*.

61

## 62 **Introduction**

63 The presence of an electron-rich sulfur sidechain makes cysteine residues extremely reactive and  
64 allows for a whole range of oxidative post-translational modifications (Reddie & Carroll, 2008).  
65 Some of these states are achieved through the initial oxidation of the free thiol group of cysteine,  
66 RSH, to RSOH (cysteine sulfenic acid). The RSOH state is very unstable and therefore can react  
67 with a second sulfenic group to generate a disulfide bridge, or RSOH oxidation can proceed to  
68 RSO<sub>2</sub>H (cysteine sulfinic acid). RSO<sub>2</sub>H may be further oxidized to yield the stable RSO<sub>3</sub>H state  
69 (cysteine sulfonic acid). Therefore, the cysteine oxidation reactions that yield cysteine sulfinic and  
70 sulfonic acid are usually considered as irreversible, while cysteine sulfenic acid may be reduced  
71 back to cysteine directly or via the formation of a disulfide bridge (Chung *et al.*, 2013).  
72 Consequently, cysteine sulfenylation by reactive oxygen species (ROS) is responsible for changes  
73 in selective interaction, enzyme activity and substrate specificity of several proteins.

74 A specific case is represented by the oxidation of N-terminal cysteinyl residues to sulfinic acid,  
75 which has been shown to promote proteasomal degradation in plants and animal cells (Hu *et al.*,  
76 2005, Graciet *et al.*, 2010). The sulfinic group supposedly mimics a carboxyl moiety of the glutamic  
77 and aspartic residues, which marks N-terminal degradation signals (N-degrons), following the  
78 pathway for proteolysis discovered by Varshavsky and colleagues (Bachmair *et al.*, 1986). Here, N-  
79 terminally exposed oxidized cysteine provides recognition specificity by the N-terminal Arg-  
80 transferase (ATE) which catalyzes Arg conjugation. This N-terminal residue, in turn, is recognized  
81 by a single subunit E3 ligase Proteolysis 6 (PRT6) that marks the protein for proteasomal  
82 degradation with a chain of polyubiquitins (Graciet & Wellmer, 2010, Tasaki *et al.*, 2012). Basal  
83 NO levels are also required to maintain the activity of this proteolytic pathway (Gibbs *et al.* 2014).

84 In plants and animals, N-terminal sulfinylation of specific proteins has been shown to be controlled  
85 by specific iron-dependent thiol dioxygenases, recently defined as N-terminal cysteine oxygenases  
86 (NCOs) (Weits *et al.*, 2014, White *et al.*, 2017, Masson *et al.* 2019). Since these enzymes use  
87 oxygen as a co-substrate, the N-degron dependent proteolysis of NCO substrates is promoted under  
88 oxic conditions and inhibited by hypoxia (Iacopino and Licausi, 2020, under revision). The first  
89 plant NCOs, Plant Cysteine Oxidases (PCOs) have been identified in Arabidopsis. Two of them,  
90 PCO1 and PCO2, have been initially identified among the proteins that constitute the core low-  
91 oxygen response (Weits *et al.*, 2014). The requirement of iron for oxygen coordination in PCOs also  
92 generate a response to fluctuations in metal availability (Dalle Carbonare *et al.* 2019). Only few  
93 Arabidopsis proteins with N-terminal cysteine have been confirmed to be substrates of the N-  
94 degron pathway: the group VII Ethylene Response Factors (ERF-VIIs), the polycomb group protein  
95 Vernalization2 (VRN2) and Little Zipper Protein ZPR2 (Gibbs *et al.* 2011, Gibbs *et al.*, 2018, Weits

96 et al., 2019). However, oxidation of ZPR2 by PCO has not been tested yet. All these transcriptional  
97 regulators regulate adaptive responses to ambient and internal oxygen fluctuations (Giuntoli et al.,  
98 2017, Weits et al., 2020, Labandera et al., 2020). Recently, a PCO-counterpart of metazoans, the  
99 Cysteamine Dioxygenase ADO, was also found to regulate stability of Methionine-Cysteine  
100 initiating proteins (Masson et al. 2019).

101 The hypoxia-inducible PCOs are not the only member of this small family: for instance in  
102 Arabidopsis three additional proteins share sequence similarity with PCO1 and PCO2, which have  
103 been subjected to biochemical characterization *in vitro* (White *et al.*, 2017, White et al. 2018).  
104 However, the role of the PCO that are not regulated by ERF-VIIs has not been elucidated *in vivo*,  
105 and the observation that they are not induced upon hypoxia suggests that they may function in  
106 different biological processes. In the present study, we filled this gap, by characterizing the role of  
107 the other PCO members with respect to hypoxia responses. We analyzed their evolutionary  
108 conservation by performing phylogenetic and functional analyses, and studied the impact of their  
109 genetic inactivation on plant physiology.

## 110 **Results**

### 111 **Protein sequence and transcriptional regulation distinguish two conserved PCO clades**

112 Whereas *PCO1* and *PCO2* are considered as part of the core anaerobic response genes in  
113 Arabidopsis (Mustroph *et al.*, 2009), the transcriptional inducibility of the other three members has  
114 not been studied in detail. We therefore tested their mRNA level in response to low oxygen  
115 conditions (1% O<sub>2</sub> V/V) in a time course over 12 h, corresponding to the light phase of the day. We  
116 confirmed that *PCO1* and *PCO2* are low-oxygen responsive, whereas no clear pattern of induction  
117 could be observed for the other three PCO genes (**Fig 1A, Supplemental Table S1, Supplemental**  
118 **Fig. 1-3**). However, previous analysis of microarray data showed that also *PCO4* is moderately  
119 induced during late hypoxia treatments (Weits *et al.*, 2014). Therefore, to further verify whether  
120 hypoxic regulation is imposed at the transcriptional level, we generated a reporter line where the  
121 expression of the beta-glucuronidase (*GUS*) gene is fused to the upstream genomic region of the  
122 *PCO4* gene, including the intergenic sequence before the start of the transcription, the 5'  
123 untranslated region (UTR) and the first 24 nt of the coding sequence (**Fig. 1b**). In seven-day old  
124 seedlings grown under aerobic conditions, GUS activity was observed in the vasculature, leaf  
125 primordia and basal zone of the first true leaves (**Fig 1b**). No increase in *PCO4prom:GUS* staining  
126 was observed after exposure to 6 h hypoxia in the dark, in either shoot or root tissues (**Fig 1b**). We  
127 therefore concluded that *PCO4*, similar to *PCO3* and *PCO5* is not induced by low oxygen  
128 conditions.

129 Next, we retrieved PCO-like sequences from angiosperm species for which the transcriptional  
130 response to low oxygen has been characterized at the whole-genome levels: Arabidopsis, rice  
131 (*Oryza sativa*), poplar (*Populus trichocarpa*), cotton (*Gossypium hirsutum*) and tomato (*Solanum*  
132 *lycopersicum*) (**Supplemental Table S2**). Since not all poplar sequences were represented on the  
133 microarray analysis available, we compared their expression level between aerobic and hypoxic (4 h  
134 1% O<sub>2</sub> v/v) conditions in a local poplar accession (*P. alba* 'Villafranca' clone). We aligned these  
135 putative orthologous amino-acid sequences and built a phylogenetic tree based on the conserved  
136 regions shared among them. The whole set of sequences separated clearly into two main clades: one  
137 (A-type PCOs) with proteins whose respective mRNA levels were not upregulated under low  
138 oxygen conditions, and a second clade (B-type PCOs) containing all low-oxygen inducible  
139 sequences (**Fig 1c, Supplemental File S1**). The two clades could be distinguished primarily due to  
140 the presence or identity of three different conserved regions within the ADO/PCO domain (interpro  
141 id IPR012864): a Glu/Asp acid triad at the beginning of the conserved (position 45-47 in AtPCO4),  
142 which is absent in the hypoxia-inducible PCOs, a substitution of Tyr with Phe/Leu towards the  
143 center of the ADO/PCO domain and the fixation of a Gly residue instead of an Ala/Thr within the  
144 highly conserved C-terminal part (**Fig. 1d**). This result hinted at a concomitant conservation of  
145 structural and cis-regulatory features for PCO genes in angiosperms.

146

#### 147 **The Hypoxia Responsive Promoter Element is conserved in the promoter of inducible PCO** 148 **genes**

149 The inducibility of B-type PCO genes by low oxygen conditions in the angiosperm species  
150 considered before is likely explained by the transcriptional regulation imposed by RAP2-type  
151 transcription factors, since this has been demonstrated in Arabidopsis previously (Gasch et al.  
152 2016). Indeed, when analyzing the 1 Kb of the 5' genomic sequence preceding the 5' untranslated  
153 region (5' UTR) of each hypoxia-inducible PCO-coding gene, we found one to four repeats of the  
154 Hypoxia Responsive Promoter Element (HRPE), identified as the main DNA feature recognized by  
155 the ERF-VII transcription factors (**Supplemental Table S2**). This 9 bp long motif occurred both in  
156 the 5' untranslated region and the upstream intergenic region. Only in the case of the  
157 *Loc\_Os1g09030* gene, the HRPE element was found inside a long 5'UTR, 1270 bp before the initial  
158 ATG codon (**Supplemental File S2**). We could not identify the same motif in the genomic region  
159 upstream of any of the A-type PCO genes. A chi-square analysis confirmed a significant correlation  
160 ( $P \leq 0.001$ ) between the occurrence of at least one HRPE element in the promoter or 5'UTR and the  
161 regulation imposed by hypoxia. These results supported the hypothesis that genes coding for B-type  
162 PCOs are controlled by ERF-VII transcription factors.

163

164 **Hypoxia-inducible B-type PCOs have been acquired and conserved in spermatophytes**

165 The identification of two separate clades of PCOs, namely A-type (not induced by hypoxia) and B-  
166 type (hypoxia inducible), led us to question when this speciation occurred during plant evolution,  
167 with possible implications in the mechanisms of oxygen perception in photosynthetic eukaryotes.  
168 We therefore searched for PCO-like sequences in genomes and transcriptomes of species belonging  
169 to taxa that could represent stepwise acquisition of traits that belong to actual angiosperms. To the  
170 angiosperm sequences used for the analysis shown in Fig. 1c before, we added those of *Pinus pinea*  
171 and *Picea abies* for gymnosperms, *Pteris vittata* and *Botrypus virginianus* for pteridophytes,  
172 *Selaginella moellendorffii* and *Lycopodium annotinum* for lycophytes, *Physcomitrella patens* and  
173 *Marchantia polymorpha* for briophytes. We also included three members of the green algae taxon:  
174 *Volvox carteri*, *Chlamydomonas reinhardtii* and *Dunaliella salina*. Reciprocal Blast-search using  
175 Arabidopsis PCOs as a reference showed that B-type sequences could only be found in  
176 spermatophytes, whereas evolutionary more primitive species only contained A-type proteins  
177 (**Supplemental Table S3**).

178 We expanded this initial analysis, by taking into consideration 212 PCO-like sequences from 42  
179 plant species whose genome has been fully sequenced, including two belonging to the rodophyta  
180 and one from the glaucophyta taxa (**Fig. 2, Supplemental Table S3**). All sequences identified  
181 contain an ADO/PCO domain, characterized by highly conserved His residues in position 98, 100  
182 (with respect to the PCO4 sequence) and, to a lesser extent, 164, which are involved in metal  
183 coordination and which are essential for dioxygenation catalysis (McCoy et al. 2006). Based on the  
184 three structural features identified above and depicted in **Fig 1d**, all PCO sequences from  
185 embryophytes could be distinguished in A-type and B-type. In few cases, highlighted in red in  
186 **Supplemental Table S3**, ambiguous attribution to either one of the two clades was solved by  
187 reciprocal blast against the Arabidopsis proteome. Algae PCO instead showed characteristics of  
188 both clades and were therefore considered as a separate one (**Fig. 2, Supplemental Table S3**). The  
189 highest number of PCO-coding genes was observed in monocots, fabales and *Malus domestica*  
190 among the rosales class, in agreement with the progression in genome size due to duplication events  
191 (Liu et al. 2016). Although the ratio B-type to A-type PCO varies considerably between species, at  
192 least one representative of both clades could be found in all spermatophytes considered. Among  
193 ferns and lycophytes, instead, only A-type PCOs were found, except for *Pteris vittata* which  
194 appeared to also contain a B-type PCO protein (**Fig. 2, Supplemental Table S3**).

195 Finally, we interrogated public sequence databases to evaluate the co-occurrence of PCOs, the other  
196 two enzymes that act in the Arg/N-degron pathway, ATE and PRT6, and established Cys-degron

197 substrates in the green lineage. We confirmed ubiquitous ATE and PRT6 presence in each  
198 examined species, although we could not always detect homologs in red algae, glaucophytes and  
199 green algae (**Fig. 2**). Cys-initiating proteins belonging to the ERF-VII group were identified in  
200 spermatophytes, including lycopods (**Fig. 2**, Supplemental Table S3), as previously indicated  
201 (Holdsworth and Gibbs, 2020). VRN2 and ZPR2 confirmed instead a later fixation in their Cys-  
202 initiating identity in angiosperms (**Fig. 2**, Supplemental Table S3Gibbs et al. 2019, Weits et al.  
203 2020).

204 We therefore speculated that the A-type PCOs represent the earliest form of plant NCO, which  
205 acquired the ability to regulate the stability of a specific ERF group in vascular plants. Moreover, in  
206 spermatophytes the B-group PCO diverged from the original clade and acquired, at the gene level,  
207 ERF-VII-dependent inducibility through the HRPE motif.

208

### 209 **Chitryds are the only fungal species with PCO-like proteins**

210 Since the existence N-terminal cysteinyl-dioxygenases (NCOs) has been confirmed in both plants  
211 and animals (Weits et al. 2014, Masson et al. 2019, Holdsworth and Gibbs 2020), we investigated  
212 their occurrence in the fungal kingdom. A thorough search throughout the proteome of fungi  
213 species whose genome has been fully sequenced returned hits only within the chytrid clade,  
214 although not all chytrid species tested showed a PCO-like sequence (**Fig. 3a, Supplemental Table**  
215 **S4, Supplemental Fig. 4**). Reciprocal identification of ADOs or PCOs in plant and metazoan  
216 databases using these fungal sequences as baits confirmed the orthology of the sequences. The  
217 presence of PCO/ADO-like sequences in almost all chytrid species in the database, but not in other  
218 phyla, can be explained as the loss of this enzymatic function in the fungal kingdom, while it was  
219 retained in chytrids. Alternatively, one can speculate about the acquisition of this enzyme  
220 exclusively by this latter fungal clade from a plant or metazoan host. We thus compared the most  
221 conserved regions identified in the ADO/PCO domain of species from the main phyla of the three  
222 kingdoms and used the resulting alignment to generate a phylogenetic tree with the Maximum  
223 Likelihood algorithm (**Fig. 3b**). Grouping of proteins reflected the assignation of original species  
224 into the three kingdoms, with chytrid putative NCOs clustering closer to plant PCOs than to  
225 metazoan ADOs (**Fig. 3b-c**). In light of this result, since speciation of Viridiplantae is estimated to  
226 have occurred before the separation of animals from fungi, we favoured the hypothesis of horizontal  
227 transfer of PCO-like gene from an ancestral green organism to a chytrid progenitor.

228

### 229 **B-type PCO conservation is extended to the transcriptional regulation**

230 Next, we investigated whether the genes encoding for B-type PCOs share conserved regulation by  
231 hypoxic conditions. Therefore, we quantified the mRNA levels of the PCO genes in one species of  
232 each taxon considered to generate the signature motifs depicted in **Fig. 1d**, selected depending on  
233 plant material available on site. Relative expression levels were monitored by realtime RT-qPCR,  
234 comparing mRNA extracted from samples exposed for different duration of hypoxic stress (1% O<sub>2</sub>  
235 v/v). Control samples were maintained in the dark and harvested at the same time of the day, to  
236 disambiguate between possible circadian regulation and true hypoxic induction. High  
237 transcriptional up-regulation by hypoxia was observed for *PCO1* of *P. pinea*, which shares the  
238 strongest sequence similarity to the hypoxia-inducible B-type PCOs of angiosperm (**Fig. 4**,  
239 **Supplemental Table S5**). On the other hand, among more ancient species, moderate up-regulation  
240 was observed for *P. vittata PCO2* and *P. patens PCO2*, although mRNA of *P. patens* followed a  
241 similar trend under aerobic conditions in darkness (**Fig. 4**). PCO-like genes belonging to *S.*  
242 *moellendorffii* and *M. polymorpha* did not show altered expression in response to hypoxia. A search  
243 for HRPE-like elements in the 5' upstream region of the *P. patens PCO2* gene did not lead to any  
244 positive identification, suggesting that its transcriptional regulation likely occurs via a different  
245 class of transcription factors or following an alternative mechanism (**Supplemental File S1**).  
246 In conclusion, our results showed that early speciation of PCO from a common eukaryotic thiol  
247 dioxygenase ancestor occurred early in the plant lineage, while hypoxic induction by ERF-VII  
248 factors was only acquired in spermatophytes, and was accompanied by specific alterations in the  
249 amino acid sequence of the PCO proteins encoded by these genes.

### 250 251 **Non hypoxia-inducible PCOs contribute to control ERF-VII stability**

252 Despite the structural differences highlighted in Fig. 3a, A-type and B-type PCOs share  
253 considerable sequence similarity among taxa, suggesting that their molecular function might be  
254 retained throughout evolution. B-type AtPCO1 and AtPCO2 have been shown to promote  
255 proteasomal degradation of ERF-VII proteins via the N-degron pathway *in vivo* and *in vitro* (Weits  
256 *et al.*, 2014, White *et al.*, 2017). We proceeded to analyze whether A-type AtPCO4 and AtPCO5 are  
257 also involved in the regulation of anaerobic responses, by controlling the stability, and thus activity,  
258 of proteins with a Cys-degron in an oxygen dependent manner. First, we tested the subcellular  
259 localization of PCO4 and PCO5: fusion to an N-terminal GFP showed nuclear and cytosolic  
260 localization, similar to what we have previously shown for PCO1 and PCO2 (**Fig. 5A**, (Weits *et al.*,  
261 2014)), independent of the occurrence of a region rich in positively charged residues typical of  
262 nuclear localization sequences (**Supplemental Table S6**). This result confirmed the potential of A-  
263 type PCOs to act on nuclear-localized transcriptional regulators. Moreover, heterologously



264 expressed PCO4 and PCO5 protein consumed molecular oxygen when incubated in the presence of  
265 a five-amino acid long CGGAI peptide, which corresponds to the N-terminal consensus of ERF-VII  
266 transcription factors (**Fig 5B**), confirming their capacity to oxidize N-terminal cysteine, as observed  
267 *in vitro* (White et al., 2018).

268 Next, we tested the ability of PCO4 and PCO5 to restrict ERF-VII activity *in vivo* by transient  
269 expression in mesophyll protoplasts. To this aim, we used the synthetic ERF-VII responsive  
270 promoter pHRPE (Kerpen et al. 2019). This was inserted in a reporter vector that bears two  
271 luciferase genes, a firefly (*Photinus pyralis*) luciferase under control of the HRPE promoter and a  
272 sea pansy (*Renilla reniformis*) luciferase driven by a 35S CaMV promoter, which was used for  
273 normalization purposes. We named this vector pHRPE-DL. Arabidopsis mesophyll protoplasts  
274 were co-transfected with pHRPE-DL, a construct designed to express the ERF-VII transcription  
275 factor RAP2.12 and either a vector bearing a PCO gene under control of the 35S promoter, or a  
276 GFP sequence as negative control. In this transient assay, PCO4 was able to repress RAP2.12  
277 activity on the HRPE promoter, while PCO5 showed only a limited, statistically non-significant  
278 effect (**Fig 5C**).

279 Finally, we examined the effect of PCO on ERF-VII stability by using a chimeric reporter protein  
280 consisting of the N-terminal 28 aa of RAP2.12 fused to firefly luciferase. To this purpose, we  
281 selected Arabidopsis lines bearing a T-DNA within the transcribed sequence of *PCO4* and *PCO5*.  
282 We first identified homozygous *pco4* and *pco5* single mutants and subsequently crossed them to  
283 generate a double *pco4/5* knock-out mutant (**Supplemental Fig. S5**). For comparison, a previously  
284 identified *pco1/2* mutant was also included in the analysis. The activity of the chimeric reporter in  
285 protoplasts was enhanced in both *pco1/2* and *pco4/5* double mutants, and we observed an even  
286 stronger RAP2.12-PpLUC signal when this reporter was expressed in a *4pco* background where  
287 both A-type and B-type PCOs are knocked-out (**Fig. 5D**). This observation indicates that both PCO  
288 clades act redundantly to regulate ERF-VII proteolysis. We also observed enhanced stability of a  
289 full-length LITTLE ZIPPER 2 (ZPR2)-firefly luciferase fusion in the *4pco* mutant, providing  
290 evidence that ZPR2 is also a PCO substrate *in vivo*. The signal of MA-initiating versions of both  
291 chimeric reporters was higher than the MC version, and comparable between the wild-type and all  
292 *pco* knock-out genotypes (**Fig. 5E**). This confirmed that proteolysis initiated by PCOs requires an  
293 N-terminally exposed cysteine, while it also indicates that additional regulation occurs at the N-  
294 terminally exposed cysteine, possibly via the remaining PCO3 enzyme. Taken together, these  
295 observations support the hypothesis that A-type PCOs also possess the ability to oxidize N-terminal  
296 exposed cysteine and, in angiosperms, both clades act to restrict the anaerobic response by  
297 promoting proteolysis of substrates of the N-degron pathway.

298

299 **In Arabidopsis, A-type PCOs play a role to repress the hypoxic response under aerobic**  
300 **conditions**

301

302 Previously, we showed that PCO1 and PCO2 repress the hypoxic response under aerobic conditions  
303 (Weits et al., 2014). Since also PCO4 and AtPCO5 are able to promote ERF-VII degradation, their  
304 inactivation would be expected to lead to an induction of the hypoxic response. We therefore aimed  
305 at discerning the contribution of each PCO clade on the regulation of the anaerobic response, by  
306 analyzing the expression of seven genes that belong to the core anaerobic response (Mustroph et al.  
307 2009) in the *pco1*, *pco2*, *pco4*, *pco5*, *pco1/2,pco4/5* and *4pco* mutants and compared their  
308 expression to that of wild type plants. The selected genes included those involved in fermentation  
309 (*Alcohol Dehydrogenase ADH*, *Pyruvate Decarboxylase PDC1*, *Sucrose Synthase SUS1* and *SUS4*  
310 (Santaniello et al., 2014)) and signaling (*Hypoxia Responsive Attenuator 1 HRA1* (Giuntoli et al.,  
311 2014) and *LOB Domain transcription factor 41 LBD41*). In adult 4-week old plants we could  
312 observe only a minor and statistically non-significant effect on the expression of these genes in the  
313 *pco1/2* and *pco4/5* mutants. Instead, the *4pco* mutant showed a significant increase in the expression  
314 of the anaerobic genes when compared to the wild-type, showing that both PCO clades act  
315 redundantly under aerobic conditions at this developmental stage (**Fig. 6A**). Comparable anaerobic  
316 gene expression was observed in *pco* mutant lines using 10-day old plants, whereas 5-day old  
317 *pco1/2* and *pco4/5* seedlings showed increased hypoxia-inducible transcripts under aerobic  
318 conditions, albeit not as strong as in the *4pco* background (**Fig. 6A**). These observations show that  
319 both PCO groups are involved in the repression of anaerobic responses and confirm the existence of  
320 age-dependent regulation imposed on the activation of anaerobic genes, as reported before (Giuntoli  
321 et al. 2017).

322 Since expression of hyper-stable versions of ERF-VII and ZPR2 caused altered plant phenotype  
323 (Giuntoli et al. 2017, Weits et al. 2020), we also characterized the consequences of PCO  
324 inactivation on development and growth. When grown in vertical plates, the high-order *pco* mutants  
325 exhibited delayed germination although this reduction was significant only for the *4pco* genotype,  
326 while the single mutants could not be distinguished from the wild type (**Fig. 6B**). Moreover, when  
327 grown in pots, *4pco* mutant adult plants developed wrinkled, pale leaves characterized by a higher  
328 degree of serration (**Fig. 6C**), while the single and double mutants remained undistinguishable from  
329 the wild type. Altogether, the gene expression and phenotypic analyses support a high degree of  
330 redundancy among PCO isoforms in controlling the anaerobic response in plants and preventing the  
331 developmental consequences of its activation under aerobic conditions.

332

### 333 **Constitutive induction of anaerobic genes in *pco4pco5* mutants affects anaerobic survival**

334

335 Constitutive activation of the anaerobic response was shown to have a negative effect on the overall  
336 ability of plants to endure actual oxygen deficiency, depending on the experimental conditions  
337 employed (Licausi *et al.*, 2011, Gibbs *et al.*, 2011, Riber *et al.*, 2015). Keeping this in mind, we  
338 tested the relevance of PCO4 and PCO5 in tolerance to temporary oxygen deficiency. We did not  
339 include the quadruple *4pco* mutant in this survey, since its pleiotropic phenotype made it extremely  
340 difficult to obtain a sufficient number of homogenous plants to be treated, and its altered growth  
341 hindered proper fitness scoring (Masson *et al.* 2019, **Fig. 6C**). Thus, we first compared the anoxic  
342 survival rate of single *pco4* and *pco5* and double *pco4/5* mutants with that of the wild type when  
343 plants were grown on a sugar-supplemented medium. In this condition, the double mutant exhibited  
344 a significant improvement in anoxic tolerance (**Fig. 7A and B**), possibly due to a primed state of  
345 acclimation to anaerobic conditions in the presence of sufficient supply of carbon for glycolysis and  
346 fermentation. Indeed, in a separate test conducted with exogenously supplemented sucrose, the  
347 *pco4/5* mutant exhibited high fermentative potential under aerobic and hypoxic conditions. In  
348 particular, it produced in air as much ethanol as the wild type after 12 h of hypoxia (**Fig. 7C**). On  
349 the other hand, we observed the opposite trend when we exposed soil-grown plants to flooding as a  
350 mean to impose oxygen deprivation: the double mutant was significantly reduced in terms of  
351 biomass production after a four-day submergence in the darkness (**Fig 7D-E**). We interpreted this  
352 result as a negative effect of enhanced fermentation when plants experience hypoxia in conditions  
353 of severe carbon limitation.

354

### 355 **Discussion**

356 In the present study, a phylogenetic analysis of the occurrence of NCO sequences among  
357 eukaryotes revealed that these are ubiquitously present in the plant kingdom (**Fig. 2**), as they are in  
358 the animal one (Masson *et al.* 2019). Sequences with high similarity to plant cysteine oxidases were  
359 fixed in embryophytes, possibly already to catalyze N-terminal cysteine oxidation, where this  
360 family proliferated due to genome duplication events. Among the classes of Cys-starting proteins  
361 identified so far in plants as PCO substrates, ERF-VIIs seem to be the earliest to be fixed in  
362 vascular plants, while ZPR2 and VRN2 proteins followed, in angiosperms (**Fig. 2**). This suggests a  
363 progressive co-adaptation with PCO to accommodate the N-terminal degron to PCO activity. It is  
364 tempting to speculate about the requirement for an ERF-VII/PCO circuit when plants acquired with  
365 vascularization a level of complexity that entails internal oxygen gradients (van Dongen and

366 Licausi, 2015). Hypoxia-responsiveness is not a conserved feature of these proteins, which we  
367 defined here as A-type PCOs. Our analysis indicates that, instead, hypoxia-inducible B-type PCOs  
368 represent a relatively recent acquisition by spermatophytes, where a second group branched out  
369 from the original family (**Fig. 1C**). The innovation of these B-type PCOs is not limited to the  
370 protein sequence, where we could identify three main signature motifs that distinguish A- and B-  
371 type PCOs (**Fig. 1D**), but also extends to the acquisition of a DNA element, in the promoter of their  
372 respective genes, that confers ERF-VII mediated regulation under hypoxia (**Supplemental Table**  
373 **3**). The conserved co-occurrence of this cis-regulatory feature and structural characteristics is  
374 suggestive of an optimization of anaerobiosis-inducible isoforms to reduced oxygen availability. In  
375 this way, B-type PCOs may play a role during hypoxia to specifically recognize ERF-VII proteins  
376 to ensure efficient and rapid restraint of anaerobic responses such as fermentation, whose excess has  
377 been shown to be detrimental for plant survival under submergence (Licausi et al. 2011, Paul et al.  
378 2016). Remarkably, the need of a similar feedback loop has also been reported for mammals. Here,  
379 the oxygen sensing enzyme Prolyl Dehydrogenases (PHDs) control the stability of the  $\alpha$  subunit of  
380 the hypoxia-inducible factor-1 (HIF1) complex, which, in turn, further upregulates PHD expression  
381 (Henze and Acker, 2010).

382 As mentioned above, NCO seem to be ubiquitously distributed and conserved in the plant and  
383 animal kingdom. Fungi, on the other hand, represent a peculiar case: we could only find NCO-like  
384 sequences in chytridiomycota, one of the early diverging lineages of this kingdom, but not in other  
385 groups (**Fig. 3A**). Not all chytrid species tested possess a PCO-like sequence, suggesting that this  
386 gene is not essential for the biology of these organisms (**Supplemental Fig. S4**). The fact that  
387 chytrids thrive in aquatic habitats, and water is necessary for the movement of chytrid zoospores,  
388 support the hypothesis of NCO-like sequences being involved in oxygen sensing in these organism  
389 (Kagami et al. 2014). In this perspective, NCO-mediated responses might help to cope with oxygen  
390 fluctuations in aquatic environments. Future characterization of fungal NCOs and their substrates,  
391 both *in vivo* and *in vitro*, will shed light on these aspects.

392 The absence of NCO-like sequences in all other groups might indicate that this has been lost early  
393 during fungal evolution, except than in chytrids, possibly because it affected fitness negatively.  
394 However, expression of plant PCO or human ADO in the budding yeast *Saccharomyces cerevisiae*  
395 did not impair cell growth, opposing the idea of toxicity of this gene in fungi (Puerta et al. 2019,  
396 Masson et al. 2019). Alternatively, horizontal gene transfer might have led to NCO fixation in  
397 chytrid genomes. Indeed, several chytrids parasitizes animal or plants species. The closest similarity  
398 of chytrid NCOs to PCOs rather than animal ADOs would favor the hypothesis of an acquisition  
399 from a plant donor (**Fig. 3B-C**). In support of this, chytrid fossils from the Rhynie chert, a

400 Devonian-age lagerstätte, are parasites of rhyniophytes, demonstrating early establishment of plant  
401 parasitism (Taylor et al. 1994).

402 As mentioned above, the A-type PCOs do not exhibit conserved responsiveness to hypoxia at the  
403 transcript level. Nevertheless, PCO4 has been confirmed as a potential initiator of the proteolytic N-  
404 end rule pathway *in vitro* (White *et al.*, 2017) and indeed could repress RAP2.12 activity in a  
405 transient assay, and inhibit the accumulation of N-degron reporters (**Fig. 5C-E**). The observation  
406 that a concomitant knocking-out of *PCO4* and *PCO5* genes induces activation of the anaerobic  
407 response in young *Arabidopsis* seedlings (**Fig. 6A**), indicates that their affinity for ERF-VII is  
408 sufficient *in vivo* to control the stability of these TFs under aerobic conditions. On the other hand, at  
409 later stages, the remaining PCO enzyme in *Arabidopsis*, or parallel repressive mechanisms, were  
410 sufficient to repress ERF-VII activity and thus induction of anaerobic genes (**Fig. 6A**). We reported  
411 similar observations for other mutants of the N-degron pathway, whose ability to further process  
412 substrates with N-terminal Cys is impaired (Giuntoli et al. 2017). Remarkably, while loss of four  
413 out of five PCO enzymes deregulates the anaerobic response, all other genotypes analyzed so far  
414 displayed some degree of complementation, suggesting the establishment of additional mechanism  
415 that restrict ERF-VII activity some days after germination. It is also interesting to note that all four  
416 PCO sequences analyzed so far can enter the nucleus (**Fig. 5A**, Weits *et al.*, 2014) irrespective of  
417 the presence of typical nuclear localization sequences, suggesting that PCOs may be imported into  
418 the nucleus by a different mechanism.

419 Assuming that one of the roles of the PCOs is to restrain the activation of fermentation under  
420 aerobic conditions, it is not surprising that their absence negatively affects plant fitness, as seen by a  
421 decrease in germination speed and shoot growth in the *4pco* mutant (**Fig. 6B-C**). It is likely that  
422 these plants are exposed to a similar metabolic stress as that identified in plants expressing a  
423 stabilized version of RAP2.12 (Paul *et al.*, 2016). Additional explanation for the *4pco* phenotype  
424 may be found via PCOs regulation on cys-degron proteins VRN2 and ZPR2, which are *in vitro* and  
425 *in vivo* PCO substrates respectively (Gibbs et al., 2018, **Fig. 5E**). VRN2 and ZPR2 regulate  
426 different aspects of plant development and accumulate in meristematic niches, tissues that have  
427 been characterized as chronically hypoxic (Gibbs et al., 2018, Shukla et al., 2019, Weits et al.,  
428 2020). Excessive abundance of these MC proteins in *4pco* mutants may therefore also play a role in  
429 causing its peculiar phenotype.

430 When single or double *pco* mutants, which do now show remarkable morphologic alterations under  
431 non-stress conditions, are challenged with oxygen deprivation, their performance strongly depends  
432 on the availability of carbon resources to support energy production via glycolysis coupled to  
433 fermentation. Indeed, double *pco4/5* mutants showed increased survival rate to anoxic exposure

434 when grown, in the presence of exogenous sucrose (**Fig. 7A-B**), whereas they exhibited impaired  
435 biomass maintenance when grown in soil and subjected to prolonged submergence (**Fig. 7D-E**). In  
436 the past, contrasting results have been obtained when comparing plants impaired in ERF-VII  
437 degradation and subjected to oxygen deprivation (Gibbs *et al.*, 2011, Licausi *et al.*, 2011). Most  
438 divergent outcomes have been reported in the case of submergence, which is a compound stress that  
439 involves several factors in addition to reduced oxygen availability (Bailey-Serres & Colmer, 2014).  
440 An extensive analysis of the possible reasons for this have been carried out by Riber and colleagues,  
441 pointing at the importance of humidity in post-submergence conditions and the content and usage of  
442 carbon reserves in the plant (Riber *et al.*, 2015). Due to the high relevance of this topic for crop  
443 breeding and farming practices, most useful and conclusive information on this matter is likely to  
444 come from the analysis of plant performance, when grown and challenged with submergence in  
445 proper agricultural conditions i.e. in open fields.

446

## 447 **Conclusions**

448 The study presented here allows for a subdivision of PCOs into two clades based on their amino  
449 acid sequence and their transcriptional regulation: those that are induced upon hypoxia (B-type) and  
450 those whose expression is unaffected by oxygen limitation (A-type). Both PCO clades are involved  
451 in the repression of the anaerobic response under normoxic conditions. Interestingly, A-type PCOs  
452 are present ubiquitously, whereas the B-type enzymes have evolved with spermatophytes. In  
453 gymnosperms and angiosperms, the hypoxia-inducible clade PCOs may therefore have evolved as a  
454 mechanism to fine-tune the extent of the anaerobic response to the strength of the hypoxic stress.  
455 The Arabidopsis proteome contains over 200 proteins with a cysteine in amino terminal position.  
456 These proteins are all potentially targets of PCOs and their identification may lead to more  
457 information on which other processes may be regulated by the oxygen-dependent branch of the N-  
458 degron pathway for protein degradation.

459

## 460 **Materials and methods**

### 461 **Plant material and growth conditions**

462 *Arabidopsis thaliana* Columbia-0 (Col-0) was used as wild-type ecotype. Single *pco4*  
463 (GABI\_740F11) knockout seeds were obtained from GABI-Kat. Single *pco5* (SALK\_128432)  
464 knockout seeds were obtained from the Nottingham Arabidopsis Stock Centre (NASC).  
465 Homozygous lines were identified via PCR screening of genomic DNA using gene-specific primers  
466 together with T-DNA-specific primers. Double homozygous lines were obtained by crossing the

467 two single mutants and then screening the F2 generation as described above. *Pinus pinea* nuts were  
468 collected along the Arno river in a 300 m<sup>2</sup> area centered around Google maps coordinates  
469 43.704733, 10.424682. *Pteris vittata* spores were collected from spontaneous plants found in the  
470 garden surrounding Casa Pacini of the Department of Crop Plants of the University of Pisa  
471 (coordinates 43.704733, 10.424682). *Selaginella moellendorffii* was purchased by Bowden Hostas  
472 and propagated vegetatively. *Physcomitrella patens* was provided by Tomas Morosinotto  
473 (University of Padova). *Marchantia polymorpha* Cam2 was provided by Linda Silvestri (University  
474 of Cambridge).

475 Growth in soil of *Arabidopsis* plants: seeds were sown in moisted soil containing pit and perlite in a  
476 3:1 ratio, stratified at 4 °C in the dark for 48 h and then germinated at 22 °C day/18 °C night with a  
477 photoperiod of 8 h light and 16 h darkness with 80-120 μmol photons m<sup>-2</sup>s<sup>-1</sup> intensity. For qPCR  
478 experiments on adult plants, 5-week-old plants were treated with low-oxygen in plexiglas box  
479 flushed with an artificial atmosphere containing nitrogen and oxygen in the proportions defined in  
480 the results section.

481 Axenic growth of *Arabidopsis* plants: seeds were sterilized using 70% ethanol for 1 min, incubated  
482 in 0.04% bleach for 10 min and rinsed six times with 1 ml distilled sterile water. Seeds were  
483 resuspended in 1 ml sterile water. Growth in liquid medium was performed inoculating 100 μl of  
484 seed suspension corresponding to 20-40 seeds in 2 ml of sterile MS medium (basal salt mixture,  
485 2.15 g l<sup>-1</sup>, pH 5.7) supplemented with 1% sucrose in each well of 6-well plates. Seeds were  
486 incubated in the dark at 4°C for 48h and subsequently germinated for four days at 22 °C day/18 °C  
487 night with a photoperiod of 12 h light and 12 h darkness. Growth on solid medium was performed  
488 in square dishes (10 cm side) containing 40 ml of solid MS medium (basal salt mixture, 2.15 g l<sup>-1</sup>,  
489 pH 5.7) supplemented with 1% sucrose and 0.8% Agar. After stratification for 48h at 4°C in the  
490 dark, germination and growth of the plants occurred at 22 °C day/18 °C night with a photoperiod of  
491 12 h light and 12 h darkness.

492 *Pinus pinea*, *Pteris vittata* and *Selaginella moellendorffii* were grown on perlite soil under growth  
493 chamber conditions as described above for *Arabidopsis thaliana*. Plantlets of *Populus alba*  
494 ‘Villafranca’ clone were maintained in in vitro conditions and treated with hypoxia as described in  
495 Dalle Carbonare et al. 2019. *Physcomitrella patens* was cultured in sterile conditions on solid Knop  
496 medium described in (Reski & Abel, 1985) while *Marchantia polymorpha* in solid MS half-strength  
497 medium (0.9% w/v Agar).

## 498 **Low oxygen treatments**

499 Plants were subjected to low oxygen treatments inside Plexiglas boxes where an artificial  
500 atmosphere containing a mixture of oxygen and nitrogen gases according to the ratios defined in the  
501 results session was continuously flushed. During the hypoxic treatments, the boxes were maintained  
502 in the dark to avoid oxygen release by photosynthesis. Individual boxes were used for each time  
503 point to avoid cycles of hypoxia and reoxygenation. Plants used for control samples were  
504 maintained in the dark for an equal amount of time. Survival rate based on emergence of new leaves  
505 was measured seven days after the exposure to anoxic conditions. Submergence was imposed to  
506 four-week old plants grown in soil as described above, inside glass tanks entirely covered with  
507 aluminum foil to maintain dark conditions. Deionized water was equilibrated for 12 h to the room  
508 temperature before pouring it slowly into the tanks up to a 15 cm from the bottom of the tank.

## 509 **Cloning of the plant and bacterial expression vectors**

510 Coding sequences and promoters were amplified from complementary cDNA or genomic DNA  
511 templates respectively using the Phusion High Fidelity DNA-polymerase (New England Biolabs).  
512 RAP2.12<sub>1-28</sub>-LUC and ZPR2-LUC gene fusions were obtained by overlapping PCR. All open  
513 reading frames were cloned into pENTR/D-TOPO (Thermo-Fisher Scientific). The resulting entry  
514 vectors were recombined into destination vectors using the LR reaction mix II (Thermo-Fisher  
515 Scientific) to obtain the novel expression vectors. A complete list and description of the  
516 oligonucleotides and destination vectors used is provided in **Supplemental Table S7** and **S8**,  
517 respectively.

## 518 **Identification of NCOs**

519 Identification of NCO protein sequences in different sequenced plant species was performed by  
520 searching the phytozome database ([www.phytozome.net](http://www.phytozome.net)). *Pteris vittata* and *Pinus pinea* sequences  
521 were retrieved from the 1000 Plants transcriptome database ([www.onekp.com](http://www.onekp.com)) and EuropeDB  
522 (<http://www.scbi.uma.es/pindb/>), respectively. Protein sequences similar to *Arabidopsis thaliana*  
523 PCO1 were retrieved using the BLAST algorithm (Atschul *et al.*, 1990). The sequences obtained in  
524 this way were subsequently aligned back against the *Arabidopsis thaliana* protein database to  
525 ensure that they represent the closest homologs of AtPCOs.

526

## 527 **Promoter analysis**



528 One kb of genomic sequences upstream of each PCO gene translation start position (ATG) was  
529 obtained either through the phytozome <https://phytozome.jgi.doe.gov/pz/portal.html>) or ensemble  
530 (<https://www.ensembl.org/index.html>) portals. When annotated, the 5' UTR region was also  
531 included in the analysis. The presence of HRPE (Gasch et al., 2016) cis-regulatory sequences was  
532 assessed using the FIMO package of MEME-suit 5.1.1 (Bailey et al., 2009). For each promoter, the  
533 number and position of HRPE elements was retrieved and noted in **Supplemental Table S3** and  
534 **Supplemental File S2**, respectively.

### 535 **Phylogenetic analysis**

536 Phylogenetic analysis was performed using MEGAX (Kumar *et al.*, 2018), by applying the  
537 Maximul Likelihood method and a JTT matrix-based model (Jones et al. 1992). To generate the  
538 phylogenetic tree, NCO protein sequences from different species were aligned using the MUSCLE  
539 algorithm (Edgar, 2004) and the initial trees were obtained by applying Neighbor-Join and BioNJ  
540 algorithms. The tree with the highest log-likelihood was selected and the bootstrap analysis (500  
541 repeats) returned the percentage of trees in which the associated taxa clustered together.

### 542 **Assessment of gene expression levels**

543 Total RNA extraction, DNase treatment, cDNA synthesis and qRT-PCR analysis was performed as  
544 described previously (Kosmacz *et al.*, 2015).

### 545 **PCO expression, purification and oxygen consumption assay**

546 The coding sequences of *PCO4* and *PCO5* were cloned into pDEST17 vector (Thermo-Fisher  
547 Scientific) to bear a construct coding for PCOs tagged by a cleavable 6-His peptide at the N  
548 terminus. Protein expression and purification was performed as described previously (Weits *et al.*,  
549 2014). Oxygen consumption by PCO4 and PCO5 proteins was determined using an optical sensor  
550 (Presens, Germany) as a measure for enzyme activity as described before (Weits *et al.*, 2014).

### 551 **Plant transformation**

552 Stable transgenic plants expressing PCO4prom:GUS, 35S:GFP:PCO4 and 35S:GFP:PCO5GFP  
553 were obtained using the floral dip method (Clough & Bent, 1998). T0 seeds were screened for  
554 kanamycin resistance to identify independent transgenic plants. T3 generation plants were used for  
555 the experiments.

## 556 **Confocal imaging**

557 For PCO-GFP imaging, the abaxial side of leaves from independently transformed plants (two  
558 weeks old) were analysed with a Leica DM6000B/SP8 confocal microscope (Leica Microsystems)  
559 using 488-nm laser light (20% laser transmissivity), PMT detection, and emission light was  
560 collected between 491 and 551 nm. Images were analysed and exported using the LAS X life  
561 science software ([www.leica-microsystems.com](http://www.leica-microsystems.com)), with an unchanged lookup table settings for each  
562 channel.

## 563 **Luciferase transactivation assay**

564 Transactivation assays were performed using a dual luciferase assay based on *Renilla reniformis*  
565 and *Photinus pyralis* luciferase enzymes. A 31 nt long sequence containing the HRPE element was  
566 retrieved from the LBD41 promoter (-364 to -331 from the initial ATG), repeated five times in  
567 tandem and fused to a minimal 35S promoter (Supplementary Information File S1). This sequence  
568 was synthesized by Geneart (Thermo Fisher Scientific), inserted into pENTR/D-topo (Thermo  
569 Fisher Scientific) and recombined into the *pGREEN800LUC* plasmid (Hellens *et al.*, 2005) using  
570 LR clonase mix II (Thermo Fisher Scientific) to generate a reporter vector 5xHRPE:PpLuc. To  
571 evaluate the effect of PCO proteins on RAP2.12-mediated activation of the 5xHRPE promoter, the  
572 effector plasmids were produced by recombining the CDS of PCOs, GFP and RAP2.12 from  
573 pENTR-D/TOPO into p2GW7 (Karimi *et al.*, 2002). Mesophyll protoplasts were prepared and  
574 transformed following the protocol by (Yoo *et al.* 2007) using three micrograms of each plasmid.  
575 Proteins were extracted from protoplasts after a 16h incubation in WI medium using 100  $\mu$ l of 1  $\times$   
576 passive lysis buffer (Promega). Luciferase activities were measured using the Dual Luciferase  
577 Reporter Assay kit (Promega) with a Glomax 20/20 (Promega).

## 578 **Quantification of ethanol production**

579 One-week old Arabidopsis seedlings were peeled from vertical plates and incubated for 12 h in 1 ml  
580 of liquid half-strength MS medium (pH 5.8) supplemented with 2% sucrose (w/v) with shaking. At  
581 the end of the light phase of the day, seedlings were treated with normoxia or anoxia (>0.01% O<sub>2</sub>  
582 V/V) for 12 h. At the end of the treatment, the medium was collected and the ethanol release per  
583 milligram of fresh weight of plant material was measured as described by Licausi *et al.* (2010).

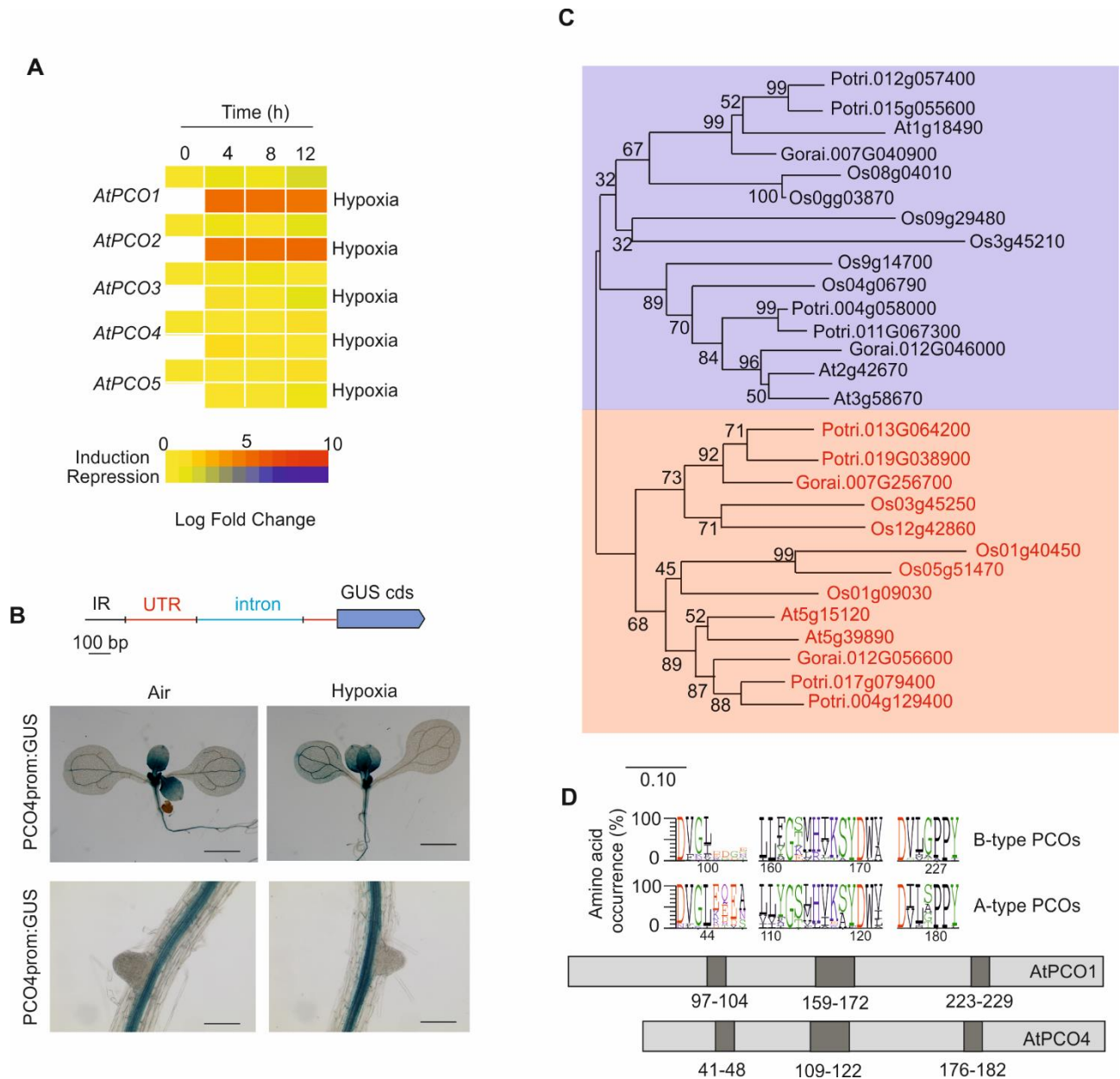
584

## 585 **Supplemental data**

- 586 Figure S1. Developmental map of *AtPCO3* expression.
- 587 Figure S2. Developmental map of *AtPCO4* expression.
- 588 Figure S3. Developmental map of *AtPCO5* expression.
- 589 Figure S4. Occurrence of NCO-like sequences in Chytrid species.
- 590 Figure S5. Genotyping of *pco4*, *pco5* and *pco4pco5* mutants.
- 591 Table S1. Relative mRNA levels of PCO genes in Arabidopsis seedlings subjected to hypoxia.
- 592 Table S2. List of PCO sequences encoded in the genome of angiosperm species for which the  
593 hypoxic transcriptome is available.
- 594 Table S3. List of PCO-like sequences identified in the genome or transcriptome of species  
595 representing evolutionary steps towards the establishment of the angiosperm taxon.
- 596 Table S4. List of NCO-like sequences identified in the chytrid group of the fungal kingdom.
- 597 Table S5. Relative mRNA levels of PCO genes in different species subjected to hypoxia.
- 598 Table S6. Identification of nuclear localization sequences within the Arabidopsis PCO proteins
- 599 Table S7. Relative mRNA levels of anaerobiosis core-response genes in *pco* Arabidopsis.
- 600 Table S8. List of primers used in this study.
- 601 Table S9. List of DNA vectors used in this study.
- 602 File S1. Occurrence of HRPE element within 5' upstream genomic sequences of PCO genes
- 603 File S2. Multialignment used to generate the phylogenetic tree used in Fig. 1C.

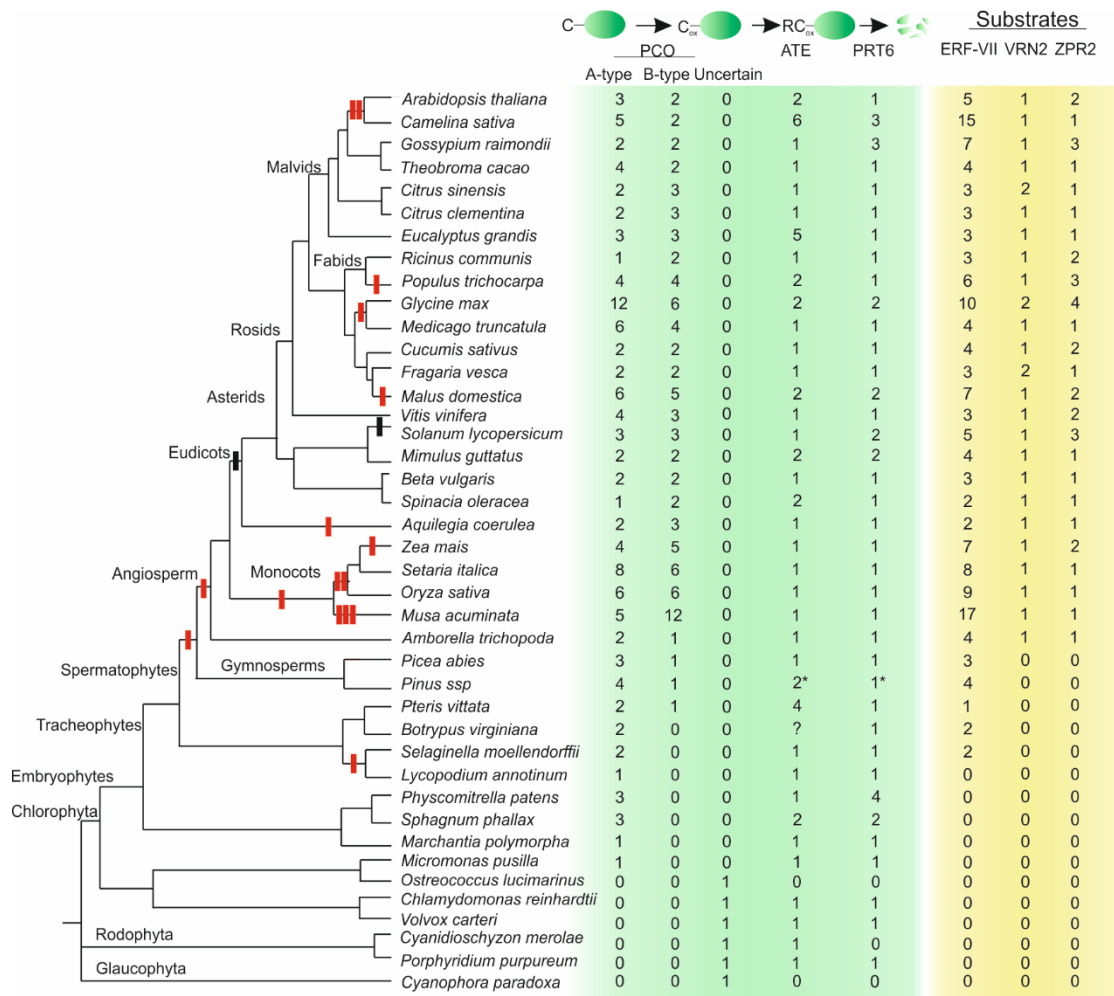
604

605 **Figures**



606  
607 **Figure 1.** Hypoxic regulation of *PCO* genes in angiosperm species. **(A)** Expression analysis of the five *PCO*  
608 genes present in the *Arabidopsis* genome in response to hypoxia. mRNA was extracted from 4-day old  
609 seedlings treated for 0, 4, 8 and 12 hours of hypoxia (1% O<sub>2</sub> v/v) and the expression of *PCOs* was compared  
610 to that of plants kept under normoxic conditions in the dark. Numeric expression values are shown in  
611 **Supplemental Table S1.** **(B)** Visualization of *PCO4* promoter activity by GUS-reporter staining in 7-day old  
612 seedlings treated with 6 h normoxia or hypoxia (1% O<sub>2</sub> v/v). **(C)** Phylogenetic tree illustrating the relatedness  
613 of *PCO* proteins encoded by angiosperms for which transcript data about low oxygen responses are  
614 available: *Arabidopsis thaliana* (*At*), *Populus trichocarpa* (*Potri*), *Oryza sativa* (*Os*), *Solanum lycopersicum*  
615 (*Sl*), and *Gossypium raimondii* (*Gorai*). The Maximum likelihood method and JTT matrix-based model was  
616 used to generate an unrooted tree of *PCOs*. Branch length represent the number of substitutions per site. The  
617 percentage of trees in which the associated isoforms clustered together is shown next to the branches. Protein  
618 sequences used for the alignment are listed in **Supplemental Table S2.** The genes that encode for the *PCOs*  
619 that were shown to be significantly upregulated upon low oxygen exposure are indicated in red (p-

620 value<0.05). **(D)** Amino acid occurrence in the three conserved regions that show the largest variation  
621 between A-type and B-type PCO clades. Their position in AtPCO1 and AtPCO4 protein is shown at the  
622 bottom of the panel. Letter height represent percentage of occurrence.  
623



624

625

626

627

628

629

630

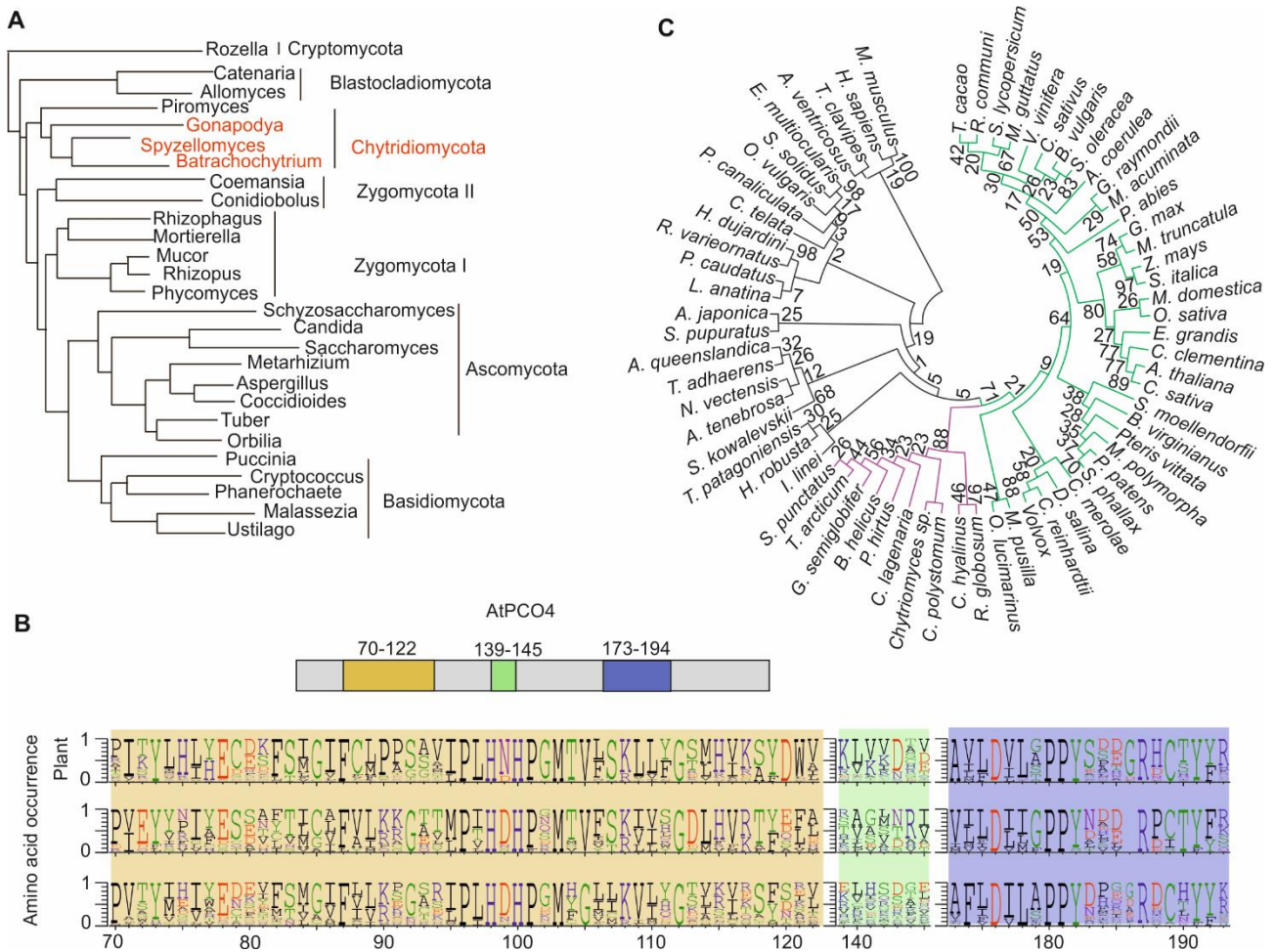
631

632

633

634

**Figure 2.** Evolutionary conservation across plant species of components of the oxygen-dependent branch of the N-degron pathway and their known targets. Whole-genome duplications are shown with vertical red bars for the branches corresponding to land plants, as described in Liu et al (2016). Vertical red ticks indicate genome duplication event, vertical black ticks represent genome triplication events. The number of non-identical sequences attributed to each class of predicted proteins and clade assignment for each PCO sequence is shown on the right side of the tree. The asterisks for ATE and PRT6 sequences in *Pinus spp* indicate that they were retrieved from the *Pinus tadea* predicted proteome, while PCO and ERF-VII sequences have been confirmed by cloning and sequencing from *Pinus pinea* mRNA. Question marks indicate identification of sequences that correspond to portions of the protein used as a bait but did not clear classification.



635

636

637

638

639

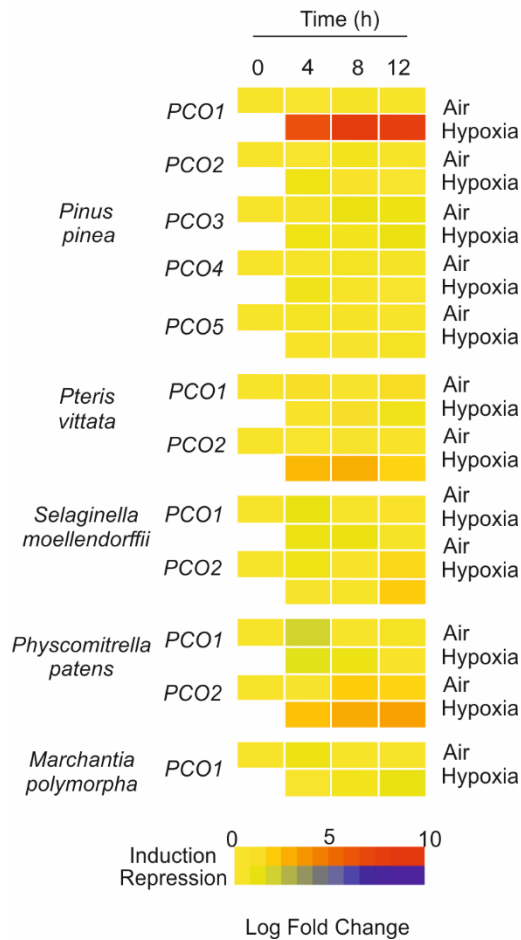
640

641

642

643

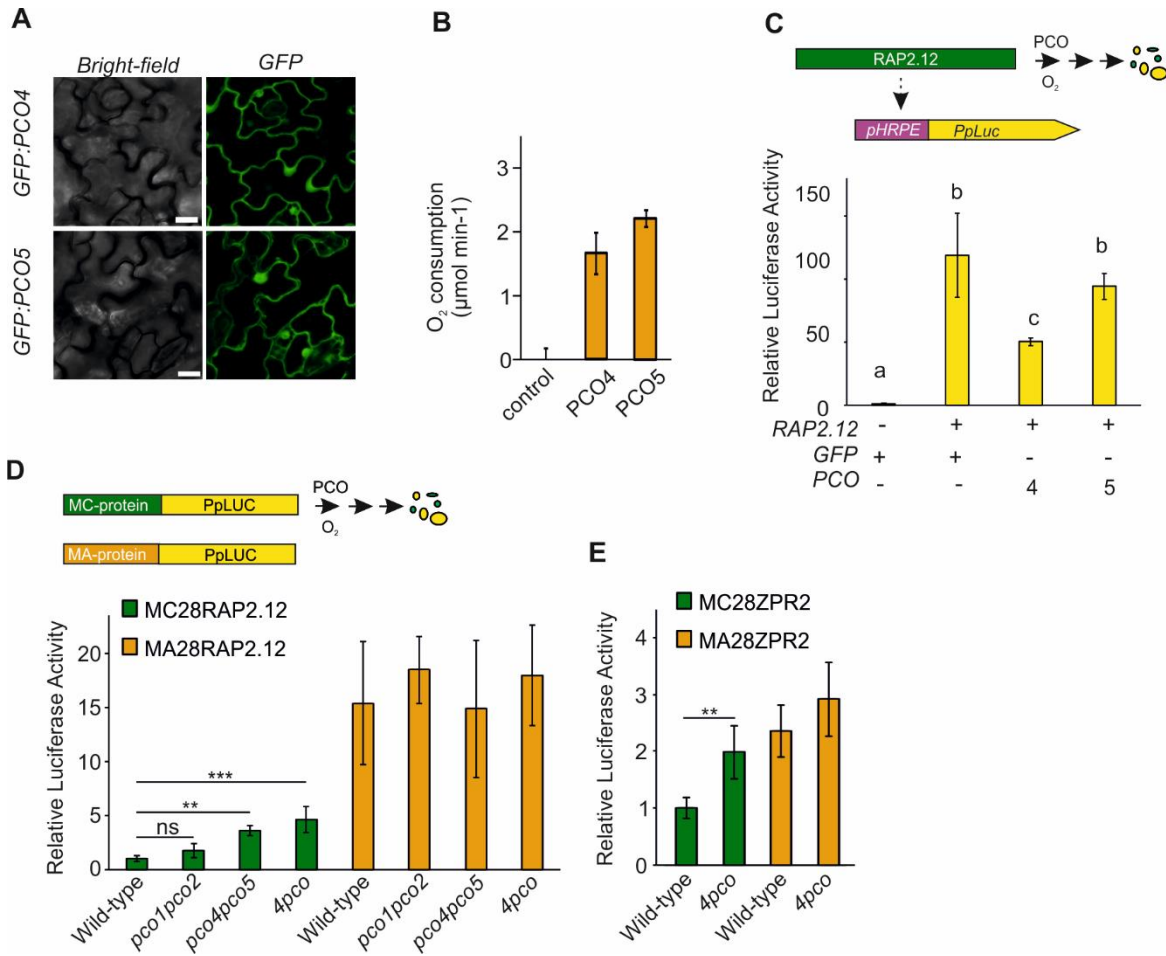
**Figure 3.** Presence of NCO-like sequences across the fungal kingdom. **(A)** The phylogeny of fungi is based on the analysis by **Chang et al. 2015**. Species whose genome contains at least one NCO-like coding gene are marked in red. **(B)** Amino acid occurrence in three conserved regions of NCOs in animals, plants and fungi. Their position in AtPCO4 protein is shown at the top of the panel. **(C)** Relatedness of NCO proteins across the three eukaryotic kingdoms (plants in green, fungi in purple and animals in black), inferred by using the Maximum Likelihood method and JTT matrix-based model. Results of the bootstrap analysis are shown next to each branch.



644

645 **Figure 4.** Expression analysis of PCOs in response to hypoxia in different plant species that represent  
 646 subsequent steps in the evolution of land plants. mRNA was extracted from samples treated for 0, 4, 8 and 12  
 647 hours of dark hypoxia (1% O<sub>2</sub> v/v) and the expression of PCOs was compared to that of plants kept under  
 648 normoxic conditions in the dark ('Air'). Numeric expression values are shown in **Supplemental Table S5**.  
 649





650

651

652

653

654

655

656

657

658

659

660

661

662

663

664

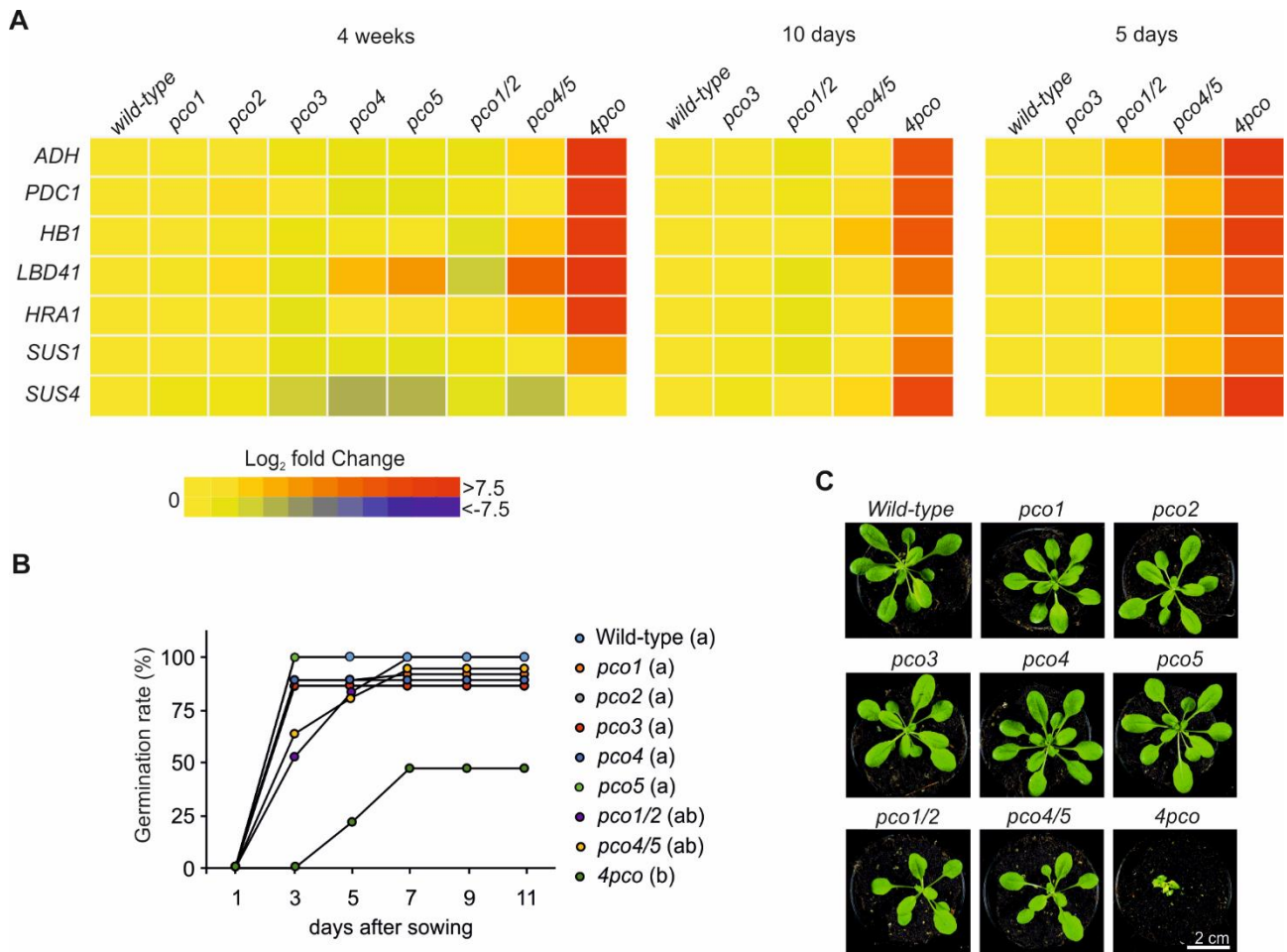
665

666

667

668

**Figure 5.** Role of A-type PCOs in controlling the activity of Cys-degron proteins. **(A)** Subcellular localization of PCO4 and PCO5 proteins harboring an N-terminally fused eGFP. Scale bars, 10 μm. **(B)** Oxygen consumption by purified PCO4 and PCO5 enzymes in a Cys oxidation *in vitro* assay using a CGGAI pentapeptide. Data are presented as mean±s.d. (n=6). Asterisks indicate statistically significant difference from a heat-inactivated protein extract as a control ( $P<0.05$ , one-way ANOVA). **(C)** Effect of *PCO4* and *PCO5* expression on transactivation imposed by RAP2.12 in *Arabidopsis thaliana* mesophyll protoplasts. To analyze RAP2.12 activity, a synthetic promoter harboring a five time repeat of the hypoxia responsive promoter element (HRPE) fused to a minimal 35S CaMV promoter driving expression of a firefly luciferase (*Photinus pyralis*) was used. A 35S:GFP vector was used as control. Data are presented as mean±s.d. (n=5). Letters indicate statistically significant difference ( $P<0.05$ , one-way ANOVA, Holm-Sidak post-hoc test). The experiment was repeated twice obtaining similar results. **(D and E)** N-degron reporter activity in plant genotypes with different PCO activity. Protoplasts of wild-type, double *pco1/2* and *pco4/5* mutants and quadruple *4pco* mutants were transiently transformed to express reporter (RAP2.12<sub>1-28</sub>-FLuc in **D** and ZPR2-FLuc in **E**) and normalizer luciferases (35S:RLuc). N-degron substrate reporters are shown in green, while stable reporters are shown in orange. Data are presented as mean±s.d. (n=5, the experiment was repeated twice). Asterisk indicate statistically significant difference (one-way ANOVA followed by Holm-Sidak post-hoc test in D, two-tailed t-test in E).



669

670

671

672

673

674

675

676

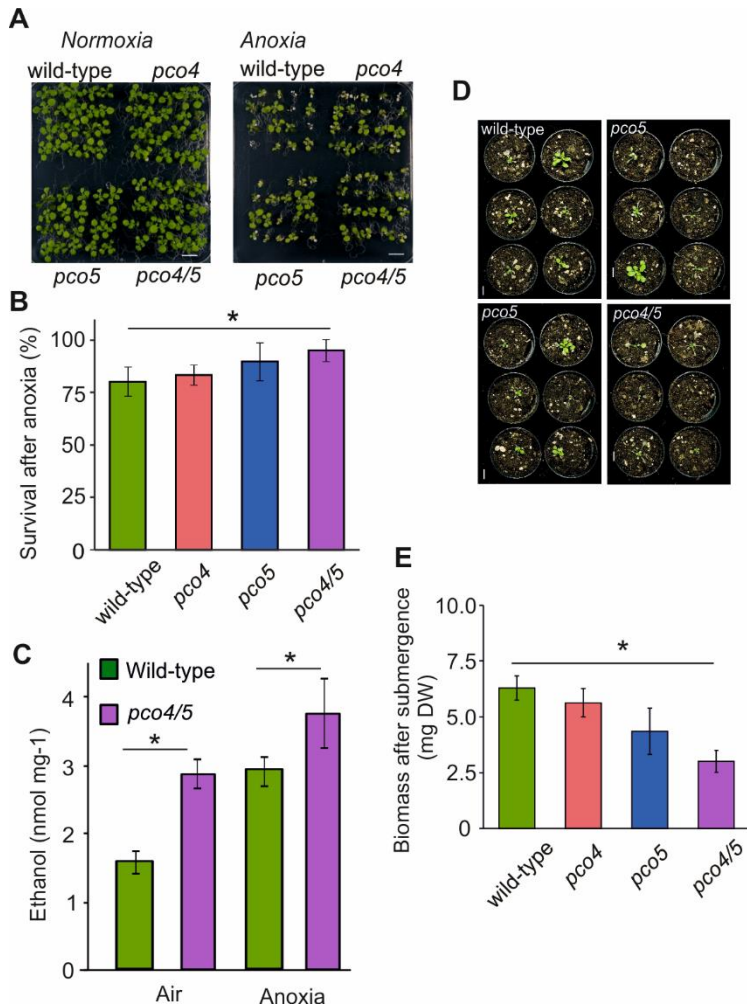
677

678

679

680

**Figure 6.** The effect of PCO knock out mutants on plant growth and the molecular response to anaerobiosis. (A) Phenotype of *pco4*, *pco5* and *pco4pco5* mutants grown on agarized MS medium. Scale-bar (A) Heat map depiction of the transcript levels of 10 genes belonging to the core set of the anaerobic response in single (*pco1*, *pco2*, *pco3*, *pco4* and *pco5*), double (*pco1/2* and *pco4/5*) and quadruple (*4pco*) mutants grown for four weeks, 10 days and 4 days under normoxic conditions. Numeric expression values are shown in **Supplemental Table S7**. (B) Germination percentage of wild-type and *pco* mutant seeds. Letters close to the genotype legend indicate grouping according to statistically significant differences. This was assessed by Kaplan-Meier Survival Analysis (Log-Rank) followed by Holm-Sidak post-hoc test. (C) Phenotype of wild-type and *pco* mutants grown in soil for four weeks. Scale bar, 1 cm.



681

682

683

684

685

686

687

688

689

690

691

692

693

**Figure 7.** Contribution of PCO4 and PCO5 to the tolerance of Arabidopsis plants to low oxygen conditions. **(A)** Phenotypes of in vitro-grown wild-type, *pco4*, *pco5* and *pco4/5* plants 7 d after exposure to 9 h of normoxia or anoxia (<0.01% O<sub>2</sub> v/v). Scale bar 1 cm. **(B)** Percentage of wild-type, *pco4*, *pco5* and *pco4pco5* plants surviving 9 h of anoxia in the dark, following a 7 d recovery period. **(C)** Ethanol production in tissues of wild-type and the double *pco4/5* mutant. One-week old plants were transferred to sterile media containing 2% (w/v) sucrose 12 h before being incubated for 12 h with anoxia or normoxia. The box plots are built on the basis of five replicates. **(D)** Phenotypes of soil-grown wild-type, *pco4*, *pco5* and *pco4pco5* plants recovering from 96 h of complete submergence in the dark. Scale bar 1 cm. **(E)** Biomass (dry weight) of wild-type, *pco4*, *pco5* and *pco4/5* plants following 7d of recovery from 96 h of dark submergence. Asterisks indicate statistically significant difference from wild type (P<0.05, one-way ANOVA).

694 **Literature cited**

- 695 **Altschul SF, Gish W, Miller W, Myers EW, Lipman DJ** (1990) Basic local alignment search  
696 tool. *J. Mol. Biol.* 215: 403-410.
- 697 **Bachmair A, Finley D, Varshavsky A** (1986) In vivo half-life of a protein is a function of its  
698 amino-terminal residue. *Science* **234**: 179-186.
- 699 **Bailey IL, Boden M, Buske FA, Martin Frith M, CE, Clementi L, Ren J, Li WW, Noble WS**  
700 (2009) MEME SUITE: Tools for Motif Discovery and Searching - PubMed. *Nucleic Acids Res* **37**:  
701 202–208
- 702 **Bailey-Serres J, Colmer TD** (2014) Plant tolerance of flooding stress – recent advances. *Plant,*  
703 *Cell & Environment* **37**: 2211-2215.
- 704 **Chang Y, Wang S, Sekimoto S, Aerts AL, Choi C, Clum A, LaButti KM, Lindquist EA, Ngan**  
705 **CY, Ohm RA, et al** (2015) Phylogenomic Analyses Indicate that Early Fungi Evolved Digesting  
706 Cell Walls of Algal Ancestors of Land Plants. *Genome Biol Evol* **7**: 1590–1601
- 707 **Chung HS, Wang SB, Venkatraman V, Murray CI, Van Eyk JE** (2013) Cysteine oxidative  
708 post-translational modifications: emerging regulation in the cardiovascular system. *Circulation*  
709 *research* **112**: 382-392.
- 710 **Clough SJ, Bent AF** (1998) Floral dip: a simplified method for *Agrobacterium*-mediated  
711 transformation of *Arabidopsis thaliana*. *The Plant Journal* **16**: 735-743.
- 712 **Dalle Carbonare LD, White MD, Shukla V, Francini A, PerataP, Flashman E, Sebastiani L,**  
713 **Licausi F** (2019) Zinc Excess Induces a Hypoxia-Like Response by Inhibiting Cysteine Oxidases in  
714 Poplar Roots. *Plant physiology*, **180**(3), 1614–1628.
- 715 **Edgar RC** (2004) MUSCLE: multiple sequence alignment with high accuracy and high throughput.  
716 *Nucleic Acids Research* **32**: 1792-1797.
- 717 **Gasch P, Fundinger M, Müller JT, Lee T, Bailey-Serres J, Mustroph A** (2016) Redundant  
718 ERF-VII Transcription Factors Bind to an Evolutionarily Conserved cis-Motif to Regulate  
719 Hypoxia-Responsive Gene Expression in *Arabidopsis*. *The Plant Cell* **28**: 160-180.
- 720 **Gibbs DJ, Lee SC, Isa NM, Gramuglia S, Fukao T, Bassel GW, Correia CS, Corbineau F,**  
721 **Theodoulou FL, Bailey-Serres J et al** (2011) Homeostatic response to hypoxia is regulated by the  
722 N-end rule pathway in plants. *Nature* **479**: 415-418.
- 723 **Gibbs DJ, Isa NM, Movahedi M, Lozano-Juste J, Mendiondo GM, Berckhan S, Marín-**  
724 **de la Rosa N, Vicente Conde J, Sousa Correia C, Pearce SP et al** (2014) Nitric Oxide Sensing in  
725 Plants Is Mediated by Proteolytic Control of Group VII ERF Transcription Factors. *Molecular Cell*  
726 **53**: 369-379.

- 727 **Gibbs DJ, Tedds HM, Labandera AM, Bailey M, White MD, Hartman S, Sprigg C, Mogg SL,**  
728 **Osborne R, Dambire C, Boeckx T, Paling Z, Voesenek LACJ, Flashman E, Holdsworth MJ**  
729 (2018) Oxygen-dependent proteolysis regulates the stability of angiosperm polycomb repressive  
730 complex 2 subunit VERNALIZATION 2. *Nat Commun.* **9**: 5438.
- 731 **Giuntoli B, Lee SC, Licausi F, Kosmacz M, Oosumi T, van Dongen JT, Bailey-Serres J,**  
732 **Perata P** (2014) A Trihelix DNA Binding Protein Counterbalances Hypoxia-Responsive  
733 Transcriptional Activation in Arabidopsis. *PLoS Biol* **12**: e1001950.
- 734 **Giuntoli B, Shukla V, Maggiorelli F, Giorgi FM, Lombardi L, Perata P, Licausi F** (2017) Age-  
735 dependent regulation of ERF-VII transcription factor activity in Arabidopsis thaliana. *Plant Cell*  
736 *Environ.* **40**: 2333-2346
- 737 **Graciet E, Mesiti F, Wellmer F** (2010) Structure and evolutionary  
738 conservation of the plant N-end rule pathway. *The Plant Journal* **61**: 741-751.
- 739 **Graciet E, Wellmer F** (2009) The plant N-end rule pathway: structure and functions. *Trends in*  
740 *Plant Science* **15**: 447-453.
- 741 **Hellens RP, Allan AC, Friel EN, Bolitho K, Grafton K, Templeton MD, Karunairetnam S,**  
742 **Gleave AP, Laing WA** (2005) Transient expression vectors for functional genomics, quantification  
743 of promoter activity and RNA silencing in plants. *Plant Methods* **1**: 13-13.
- 744 **Henze A, Acker T** (2010) Feedback Regulators of Hypoxia-Inducible Factors and Their Role in  
745 Cancer Biology. *Cell cycle* **14**: 2749–2763
- 746 **Holdsworth MJ, Gibbs DJ** (2020) Comparative Biology of Oxygen Sensing in Plants and  
747 Animals. *Curr Biol* **30**: R362–R369
- 748 **Hu RG, Sheng J, Qi X, Xu Z, Takahashi TT, Varshavsky A** (2005) The N-end rule pathway as a  
749 nitric oxide sensor controlling the levels of multiple regulators. *Nature* **437**: 981-986.
- 750 **Jones DT, Taylor WR, Thornton JM** (1992) The Rapid Generation of Mutation Data Matrices  
751 From Protein Sequences - PubMed. *Comput Appl Biosci* **8**: 275–282
- 752 **Kagami M, Miki T, Takimoto G** (2014) Mycoloop: Chytrids in aquatic food webs. *Front*  
753 *Microbiol* **5**: 166
- 754 **Karimi M, Inzé D, Depicker A** (2002) GATEWAY® vectors for Agrobacterium-  
755 mediated plant transformation. *Trends in Plant Science* **7**: 193-195.
- 756 **Kerpen L, Niccolini L, Licausi F, van Dongen JT, Weits DA** (2019) Hypoxic Conditions in  
757 Crown Galls Induce Plant Anaerobic Responses That Support Tumor Proliferation. *Front Plant Sci.*  
758 **10**:56.
- 759 **Kosmacz M, Parlanti S, Schwarzlaender M, Kragler F, Licausi F, Van Dongen JT** (2015) The  
760 stability and nuclear localization of the transcription factor RAP2.12 are dynamically regulated by  
761 oxygen concentration. *Plant, Cell & Environment* **38**: 1094-1103.

- 760 **Kumar S, Stecher G, Li M, Knyaz C, Tamura K** (2018) MEGA X: Molecular Evolutionary  
761 Genetics Analysis across Computing Platforms | Molecular Biology and Evolution. *Mol Biol Evol*  
762 35: 1547–1549
- 763 **Labandera AM, Tedds HM, Bailey M, Sprigg C, Etherington RD, Akintewe O, Kalleechurn**  
764 **G, Holdsworth MJ, Gibbs DJ** (2020) The PRT6 N-degron pathway restricts VERNALIZATION 2  
765 to endogenous hypoxic niches to modulate plant development. *New Phytol.* doi:  
766 10.1111/nph.16477.
- 767 **Licausi F, van Dongen JT, Giuntoli B, Novi G, Santaniello A, Geigenberger P, Perata P** (2010)  
768 HRE1 and HRE2, two hypoxia-inducible ethylene response factors, affect anaerobic responses in  
769 *Arabidopsis thaliana*. *Plant J* **62**: 302–15
- 770 **Licausi F, Kosmacz M, Weits DA, Giuntoli B, Giorgi FM, Voesenek LACJ, Perata P, van**  
771 **Dongen JT** (2011) Oxygen sensing in plants is mediated by an N-end rule pathway for protein  
772 destabilization. *Nature* **479**: 419-422.
- 773 **Liu YY, Yang KZ, Wei XX, Wang XQ** (2016) Revisiting the phosphatidylethanolamine-binding  
774 protein (PEBP) gene family reveals cryptic FLOWERING LOCUS T gene homologs in  
775 gymnosperms and sheds new light on functional evolution. *New Phytol* 212: 730–744
- 776 **Masson N, Keeley TP, Giuntoli B, White MD, Puerta ML, Perata P, Hopkinson RJ, Flashman**  
777 **E, Licausi F, Ratcliffe PJ** (2019) Conserved N-terminal cysteine dioxygenases transduce responses  
778 to hypoxia in animals and plants. *Science* **365**: 65-69
- 779 **McCoy JG, Bailey LJ, Bitto E, Bingman CA, Aceti DJ, Fox BG, Phillips GN** (2006) Structure  
780 and mechanism of mouse cysteine dioxygenase. *Proc Natl Acad Sci U S A* **103**: 3084–3089
- 781 **Mustroph, A, Zanetti ME, Jang CJH, Holtan HE, Repetti PP, Galbraith DW, Girke T, Bailey-**  
782 **Serres J** (2009) Profiling translomes of discrete cell populations resolves altered cellular priorities  
783 during hypoxia in *Arabidopsis*. *Proceedings of the National Academy of Sciences* **106**: 18843-  
784 18848.
- 785 **Paul MV, Iyer S, Amerhauser C, Lehmann M, van Dongen JT, Geigenberger P** (2016)  
786 RAP2.12 oxygen sensing regulates plant metabolism and performance under both normoxia and  
787 hypoxia. *Plant Physiology*. **172**:141-53.
- 788 **Puerta ML, Shukla V, Dalle Carbonare L, Weits DA, Perata P, Licausi F, Giuntoli B** (2019)  
789 A Ratiometric Sensor Based on Plant N-Terminal Degrons Able to Report Oxygen Dynamics in  
790 *Saccharomyces cerevisiae*. *JMB* 431: 2810-2820
- 791 **Reddie KG, Carroll KS** (2008) Expanding the functional diversity of proteins through cysteine  
792 oxidation. *Current Opinion in Chemical Biology* **12**: 746-754.

- 793 **Reski R, Abel WO** (1985) Induction of budding on chloronemata and caulonemata of the moss,  
794 *Physcomitrella patens*, using isopentenyladenine. *Planta* **165**: 354-358.
- 795 **Riber W, Müller JT, Visser EJ, Sasidharan R, Voeselek LA, Mustroph A** (2015) The Greening  
796 after Extended Darkness Is an N-End Rule Pathway Mutant with High Tolerance to Submergence  
797 and Starvation. *Plant Physiology* **167**: 1616-1629.
- 798 **Santaniello A, Loreti E, Gonzali S, Novi G, Perata P** (2014) A reassessment of the role of  
799 sucrose synthase in the hypoxic sucrose-ethanol transition in *Arabidopsis*. *Plant, Cell &*  
800 *Environment* **37**: 2294-2302.
- 801 **Shukla V, Lombardi L, Iacopino S, Pencik A, Novak O, Perata P, Giuntoli B, Licausi F** (2019)  
802 Endogenous Hypoxia in Lateral Root Primordia Controls Root Architecture by Antagonizing Auxin  
803 Signaling in *Arabidopsis*. *Mol Plant* **12**: 538–551
- 804 **Tasaki T, Sriram SM, Park KS, Kwon YT** (2012) The N-End Rule Pathway. *Annual review of*  
805 *biochemistry* **81**: 261-289.
- 806 **Taylor TN, Remy W, Hass H** (1994) *Allomyces* in the Devonian. *Nature* **367**: 601
- 807 **Weits DA, Giuntoli B, Kosmacz M, Parlanti S, Hubberten HM, Riegler H, Hoefgen R, Perata**  
808 **P, van Dongen JT and Licausi F** (2014) Plant cysteine oxidases control the oxygen-dependent  
809 branch of the N-end-rule pathway. *Nat Commun* **5**.
- 810 **Van Dongen JT and Licausi F** (2015) Oxygen Sensing and Signaling. *Annu Rev Plant Biol* **66**:  
811 345-67
- 812 **Weits DA, Kunkowska AB, Kamps NCW, Portz KMS, Packbier NK, Nemeček Z,**  
813 **Gaillochet C, Lohmann JU, Pedersen O, van Dongen JT, Licausi F** (2019) An apical hypoxic  
814 niche sets the pace of shoot meristem activity. *Nature* **569**: 714-717.
- 815 **Weits DA, van Dongen JT and Licausi F** (2020) Molecular oxygen as a signaling component in  
816 plant development. *New Phytol*. doi:10.1111/nph.16424.
- 817 **White MD, Klecker M, Hopkinson RJ, Weits DA, Mueller C, Naumann C, O'Neill R,**  
818 **Wickens J, Yang J, Brooks-Bartlett JC, et al.** (2017) Plant cysteine oxidases are dioxygenases  
819 that directly enable arginyl transferase-catalysed arginylation of N-end rule targets. *Nat Commun*  
820 **8**: 14690.
- 821 **White MD, Kamps JJAG, East S, Taylor KLJ, Flashman E** (2018) The Plant Cysteine Oxidases  
822 from *Arabidopsis thaliana* are kinetically tailored to act as oxygen sensors. *JBC* **293**, 11786-11795.
- 823 **Yoo SD, Cho YH, Sheen J** (2007) *Arabidopsis* mesophyll protoplasts: a versatile cell system for  
824 transient gene expression analysis. *Nat. Protocols* **2**: 1565-1572.

## Parsed Citations

**Aitschul SF, Gish W, Miller W, Myers EW, Lipman DJ (1990)** Basic local alignment search tool. *J. Mol. Biol.* 215: 403-410.

Pubmed: [Author and Title](#)

Google Scholar: [Author Only](#) [Title Only](#) [Author and Title](#)

**Bachmair A, Finley D, Varshavsky A (1986)** In vivo half-life of a protein is a function of its amino-terminal residue. *Science* 234: 179-186.

Pubmed: [Author and Title](#)

Google Scholar: [Author Only](#) [Title Only](#) [Author and Title](#)

**Bailey IL, Boden M, Buske FA, Martin Frith M, CE, Clementi L, Ren J, Li WW, Noble WS (2009)** MEME SUITE: Tools for Motif Discovery and Searching - PubMed. *Nucleic Acids Res* 37: 202–208

Pubmed: [Author and Title](#)

Google Scholar: [Author Only](#) [Title Only](#) [Author and Title](#)

**Bailey-Serres J, Colmer TD (2014)** Plant tolerance of flooding stress – recent advances. *Plant, Cell & Environment* 37: 2211-2215.

Pubmed: [Author and Title](#)

Google Scholar: [Author Only](#) [Title Only](#) [Author and Title](#)

**Chang Y, Wang S, Sekimoto S, Aerts AL, Choi C, Clum A, LaButti KM, Lindquist EA, Ngan CY, Ohm RA, et al (2015)** Phylogenomic Analyses Indicate that Early Fungi Evolved Digesting Cell Walls of Algal Ancestors of Land Plants. *Genome Biol Evol* 7: 1590–1601

Pubmed: [Author and Title](#)

Google Scholar: [Author Only](#) [Title Only](#) [Author and Title](#)

**Chung HS, Wang SB, Venkatraman V, Murray CI, Van Eyk JE (2013)** Cysteine oxidative post-translational modifications: emerging regulation in the cardiovascular system. *Circulation research* 112: 382-392.

Pubmed: [Author and Title](#)

Google Scholar: [Author Only](#) [Title Only](#) [Author and Title](#)

**Clough SJ, Bent AF (1998)** Floral dip: a simplified method for *Agrobacterium*-mediated transformation of *Arabidopsis thaliana*. *The Plant Journal* 16: 735-743.

Pubmed: [Author and Title](#)

Google Scholar: [Author Only](#) [Title Only](#) [Author and Title](#)

**Dalle Carbonare LD, White MD, Shukla V, Francini A, Perata P, Flashman E, Sebastiani L, Licausi F (2019)** Zinc Excess Induces a Hypoxia-Like Response by Inhibiting Cysteine Oxidases in Poplar Roots. *Plant physiology*, 180(3), 1614–1628.

Pubmed: [Author and Title](#)

Google Scholar: [Author Only](#) [Title Only](#) [Author and Title](#)

**Edgar RC (2004)** MUSCLE: multiple sequence alignment with high accuracy and high throughput. *Nucleic Acids Research* 32: 1792-1797.

Pubmed: [Author and Title](#)

Google Scholar: [Author Only](#) [Title Only](#) [Author and Title](#)

**Gasch P, Fundinger M, Müller JT, Lee T, Bailey-Serres J, Mustroph A (2016)** Redundant ERF-VII Transcription Factors Bind to an Evolutionarily Conserved cis-Motif to Regulate Hypoxia-Responsive Gene Expression in *Arabidopsis*. *The Plant Cell* 28: 160-180.

Pubmed: [Author and Title](#)

Google Scholar: [Author Only](#) [Title Only](#) [Author and Title](#)

**Gibbs DJ, Lee SC, Isa NM, Gramuglia S, Fukao T, Bassel GW, Correia CS, Corbineau F, Theodoulou FL, Bailey-Serres J et al (2011)** Homeostatic response to hypoxia is regulated by the N-end rule pathway in plants. *Nature* 479: 415-418.

Pubmed: [Author and Title](#)

Google Scholar: [Author Only](#) [Title Only](#) [Author and Title](#)

**Gibbs DJ, Isa NM, Movahedi M, Lozano-Juste J, Mendiondo GM, Berckhan S, Marin-de la Rosa N, Vicente Conde J, Sousa Correia C, Pearce SP et al (2014)** Nitric Oxide Sensing in Plants Is Mediated by Proteolytic Control of Group VII ERF Transcription Factors. *Molecular Cell* 53: 369-379.

Pubmed: [Author and Title](#)

Google Scholar: [Author Only](#) [Title Only](#) [Author and Title](#)

**Gibbs DJ, Tedds HM, Labandera AM, Bailey M, White MD, Hartman S, Sprigg C, Mogg SL, Osborne R, Dambire C, Boeckx T, Paling Z, Voesenek LACJ, Flashman E, Holdsworth MJ (2018)** Oxygen-dependent proteolysis regulates the stability of angiosperm polycomb repressive complex 2 subunit VERNALIZATION 2. *Nat Commun.* 9: 5438.

Pubmed: [Author and Title](#)

Google Scholar: [Author Only](#) [Title Only](#) [Author and Title](#)

**Giuntoli B, Lee SC, Licausi F, Kosmacz M, Oosumi T, van Dongen JT, Bailey-Serres J, Perata P (2014)** A Trihelix DNA Binding Protein Counterbalances Hypoxia-Responsive Transcriptional Activation in *Arabidopsis*. *PLoS Biol* 12: e1001950.

Pubmed: [Author and Title](#)

Google Scholar: [Author Only](#) [Title Only](#) [Author and Title](#)

**Giuntoli B, Shukla V, Maggiorelli F, Giorgi FM, Lombardi L, Perata P, Licausi F (2017)** Age-dependent regulation of ERF-VII transcription factor activity in *Arabidopsis thaliana*. *Plant Cell Environ.* 40: 2333-2346

Pubmed: [Author and Title](#)



Google Scholar: [Author Only](#) [Title Only](#) [Author and Title](#)

**Graciet E, Mesiti F, Wellmer F (2010) Structure and evolutionary conservation of the plant N-end rule pathway. The Plant Journal 61: 741-751.**

Pubmed: [Author and Title](#)

Google Scholar: [Author Only](#) [Title Only](#) [Author and Title](#)

**Graciet E, Wellmer F (2009) The plant N-end rule pathway: structure and functions. Trends in Plant Science 15: 447-453.**

Pubmed: [Author and Title](#)

Google Scholar: [Author Only](#) [Title Only](#) [Author and Title](#)

**Hellens RP, Allan AC, Friel EN, Bolitho K, Grafton K, Templeton MD, Karunairetnam S, Gleave AP, Laing WA (2005) Transient expression vectors for functional genomics, quantification of promoter activity and RNA silencing in plants. Plant Methods 1: 13-13.**

Pubmed: [Author and Title](#)

Google Scholar: [Author Only](#) [Title Only](#) [Author and Title](#)

**Henze A, Acker T (2010) Feedback Regulators of Hypoxia-Inducible Factors and Their Role in Cancer Biology. Cell cycle 14: 2749-2763**

Pubmed: [Author and Title](#)

Google Scholar: [Author Only](#) [Title Only](#) [Author and Title](#)

**Holdsworth MJ, Gibbs DJ (2020) Comparative Biology of Oxygen Sensing in Plants and Animals. Curr Biol 30: R362-R369**

Pubmed: [Author and Title](#)

Google Scholar: [Author Only](#) [Title Only](#) [Author and Title](#)

**Hu RG, Sheng J, Qi X, Xu Z, Takahashi TT, Varshavsky A (2005) The N-end rule pathway as a nitric oxide sensor controlling the levels of multiple regulators. Nature 437: 981-986.**

Pubmed: [Author and Title](#)

Google Scholar: [Author Only](#) [Title Only](#) [Author and Title](#)

**Jones DT, Taylor WR, Thornton JM (1992) The Rapid Generation of Mutation Data Matrices From Protein Sequences - PubMed. Comput Appl Biosci 8: 275-282**

Pubmed: [Author and Title](#)

Google Scholar: [Author Only](#) [Title Only](#) [Author and Title](#)

**Kagami M, Miki T, Takimoto G (2014) Mycoloop: Chytrids in aquatic food webs. Front Microbiol 5: 166**

Pubmed: [Author and Title](#)

Google Scholar: [Author Only](#) [Title Only](#) [Author and Title](#)

**Karimi M, Inzé D, Depicker A (2002) GATEWAY® vectors for Agrobacterium-mediated plant transformation. Trends in Plant Science 7: 193-195.**

Pubmed: [Author and Title](#)

Google Scholar: [Author Only](#) [Title Only](#) [Author and Title](#)

**Kerpen L, Niccolini L, Licausi F, van Dongen JT, Weits DA (2019) Hypoxic Conditions in Crown Galls Induce Plant Anaerobic Responses That Support Tumor Proliferation. Front Plant Sci. 10:56.**

Pubmed: [Author and Title](#)

Google Scholar: [Author Only](#) [Title Only](#) [Author and Title](#)

**Kosmacz M, Parlanti S, Schwarzlaender M, Kragler F, Licausi F, Van Dongen JT (2015) The stability and nuclear localization of the transcription factor RAP2.12 are dynamically regulated by oxygen concentration. Plant, Cell & Environment 38: 1094-1103.**

Pubmed: [Author and Title](#)

Google Scholar: [Author Only](#) [Title Only](#) [Author and Title](#)

**Kumar S, Stecher G, Li M, Knyaz C, Tamura K (2018) MEGAX: Molecular Evolutionary Genetics Analysis across Computing Platforms | Molecular Biology and Evolution. Mol Biol Evol 35: 1547-1549**

Pubmed: [Author and Title](#)

Google Scholar: [Author Only](#) [Title Only](#) [Author and Title](#)

**Labandera AM, Tedds HM, Bailey M, Sprigg C, Etherington RD, Akintewe O, Kalleechurn G, Holdsworth MJ, Gibbs DJ (2020) The PRT6 N-degron pathway restricts VERNALIZATION 2 to endogenous hypoxic niches to modulate plant development. New Phytol. doi: 10.1111/nph.16477.**

Pubmed: [Author and Title](#)

Google Scholar: [Author Only](#) [Title Only](#) [Author and Title](#)

**Licausi F, van Dongen JT, Giuntoli B, Novi G, Santaniello A, Geigenberger P, Perata P (2010) HRE1 and HRE2, two hypoxia-inducible ethylene response factors, affect anaerobic responses in Arabidopsis thaliana. Plant J 62: 302-15**

Pubmed: [Author and Title](#)

Google Scholar: [Author Only](#) [Title Only](#) [Author and Title](#)

**Licausi F, Kosmacz M, Weits DA, Giuntoli B, Giorgi FM, Voesenek LACJ, Perata P, van Dongen JT (2011) Oxygen sensing in plants is mediated by an N-end rule pathway for protein destabilization. Nature 479: 419-422.**

Pubmed: [Author and Title](#)

Google Scholar: [Author Only](#) [Title Only](#) [Author and Title](#)

**Liu YY, Yang KZ, Wei XX, Wang XQ (2016) Revisiting the phosphatidylethanolamine-binding protein (PEBP) gene family reveals cryptic**

**FLOWERING LOCUS T** gene homologs in gymnosperms and sheds new light on functional evolution. *New Phytol* 212: 730–744

Pubmed: [Author and Title](#)

Google Scholar: [Author Only Title Only Author and Title](#)

**Masson N, Keeley TP, Giuntoli B, White MD, Puerta ML, Perata P, Hopkinson RJ, Flashman E, Licausi F, Ratcliffe PJ (2019) Conserved N-terminal cysteine dioxygenases transduce responses to hypoxia in animals and plants. *Science* 365: 65–69**

Pubmed: [Author and Title](#)

Google Scholar: [Author Only Title Only Author and Title](#)

**McCoy JG, Bailey LJ, Bitto E, Bingman CA, Aceti DJ, Fox BG, Phillips GN (2006) Structure and mechanism of mouse cysteine dioxygenase. *Proc Natl Acad Sci U S A* 103: 3084–3089**

Pubmed: [Author and Title](#)

Google Scholar: [Author Only Title Only Author and Title](#)

**Mustroph, A, Zanetti ME, Jang CJH, Holtan HE, Repetti PP, Galbraith DW, Girke T, Bailey-Serres J (2009) Profiling transcriptomes of discrete cell populations resolves altered cellular priorities during hypoxia in *Arabidopsis*. *Proceedings of the National Academy of Sciences* 106: 18843–18848.**

Pubmed: [Author and Title](#)

Google Scholar: [Author Only Title Only Author and Title](#)

**Paul MV, Iyer S, Amerhauser C, Lehmann M, van Dongen JT, Geigenberger P (2016) RAP2.12 oxygen sensing regulates plant metabolism and performance under both normoxia and hypoxia. *Plant Physiology*. 172:141–53.**

Pubmed: [Author and Title](#)

Google Scholar: [Author Only Title Only Author and Title](#)

**Puerta ML, Shukla V, Dalle Carbonare L, Weits DA, Perata P, Licausi F, Giuntoli B (2019) A Ratiometric Sensor Based on Plant N-Terminal Degrons Able to Report Oxygen Dynamics in *Saccharomyces cerevisiae*. *JMB* 431: 2810–2820**

Pubmed: [Author and Title](#)

Google Scholar: [Author Only Title Only Author and Title](#)

**Reddie KG, Carroll KS (2008) Expanding the functional diversity of proteins through cysteine oxidation. *Current Opinion in Chemical Biology* 12: 746–754.**

Pubmed: [Author and Title](#)

Google Scholar: [Author Only Title Only Author and Title](#)

**Reski R, Abel WO (1985) Induction of budding on chloronemata and caulonemata of the moss, *Physcomitrella patens*, using isopentenyladenine. *Planta* 165: 354–358.**

Pubmed: [Author and Title](#)

Google Scholar: [Author Only Title Only Author and Title](#)

**Riber W, Müller JT, Visser EJ, Sasidharan R, Voesenek LA, Mustroph A (2015) The Greening after Extended Darkness1 Is an N-End Rule Pathway Mutant with High Tolerance to Submergence and Starvation. *Plant Physiology* 167: 1616–1629.**

Pubmed: [Author and Title](#)

Google Scholar: [Author Only Title Only Author and Title](#)

**Santaniello A, Loreti E, Gonzali S, Novi G, Perata P (2014) A reassessment of the role of sucrose synthase in the hypoxic sucrose-ethanol transition in *Arabidopsis*. *Plant, Cell & Environment* 37: 2294–2302.**

Pubmed: [Author and Title](#)

Google Scholar: [Author Only Title Only Author and Title](#)

**Shukla V, Lombardi L, Iacopino S, Pencik A, Novak O, Perata P, Giuntoli B, Licausi F (2019) Endogenous Hypoxia in Lateral Root Primordia Controls Root Architecture by Antagonizing Auxin Signaling in *Arabidopsis*. *Mol Plant* 12: 538–551**

Pubmed: [Author and Title](#)

Google Scholar: [Author Only Title Only Author and Title](#)

**Tasaki T, Sriram SM, Park KS, Kwon YT (2012) The N-End Rule Pathway. *Annual review of biochemistry* 81: 261–289.**

Pubmed: [Author and Title](#)

Google Scholar: [Author Only Title Only Author and Title](#)

**Taylor TN, Remy W, Hass H (1994) *Allomyces* in the Devonian. *Nature* 367: 601**

Pubmed: [Author and Title](#)

Google Scholar: [Author Only Title Only Author and Title](#)

**Weits DA, Giuntoli B, Kosmacz M, Parlanti S, Hubberten HM, Riegler H, Hoefgen R, Perata P, van Dongen JT and Licausi F (2014) Plant cysteine oxidases control the oxygen-dependent branch of the N-end-rule pathway. *Nat Commun* 5.**

Pubmed: [Author and Title](#)

Google Scholar: [Author Only Title Only Author and Title](#)

**Van Dongen JT and Licausi F (2015) Oxygen Sensing and Signaling. *Annu Rev Plant Biol* 66: 345–67**

Pubmed: [Author and Title](#)

Google Scholar: [Author Only Title Only Author and Title](#)

**Weits DA, Kunkowska AB, Kamps NCW, Portz KMS, Packbier NK, Nemeč VENZA Z, Gaillochet C, Lohmann JU, Pedersen O, van Dongen JT, Licausi F (2019) An apical hypoxic niche sets the pace of shoot meristem activity. *Nature* 569: 714–717.**

Pubmed: [Author and Title](#)

Google Scholar: [Author Only](#) [Title Only](#) [Author and Title](#)

**Weits DA, van Dongen JT and Licausi F (2020) Molecular oxygen as a signaling component in plant development. *New Phytol.* doi:10.1111/nph.16424.**

Pubmed: [Author and Title](#)

Google Scholar: [Author Only](#) [Title Only](#) [Author and Title](#)

**White MD, Klecker M, Hopkinson RJ, Weits DA, Mueller C, Naumann C, O'Neill R, Wickens J, Yang J, Brooks-Bartlett JC, et al. (2017) Plant cysteine oxidases are dioxygenases that directly enable arginyl transferase-catalysed arginylation of N-end rule targets. *Nat Commun* 8: 14690.**

Pubmed: [Author and Title](#)

Google Scholar: [Author Only](#) [Title Only](#) [Author and Title](#)

**White MD, Kamps JJAG, East S, Taylor KLJ, Flashman E (2018) The Plant Cysteine Oxidases from *Arabidopsis thaliana* are kinetically tailored to act as oxygen sensors. *JBC* 293, 11786-11795.**

Pubmed: [Author and Title](#)

Google Scholar: [Author Only](#) [Title Only](#) [Author and Title](#)

**Yoo SD, Cho YH, Sheen J (2007) *Arabidopsis* mesophyll protoplasts: a versatile cell system for transient gene expression analysis. *Nat. Protocols* 2: 1565-1572.**

Pubmed: [Author and Title](#)

Google Scholar: [Author Only](#) [Title Only](#) [Author and Title](#)